«ФИЗИКА ЭЛЕМЕНТАРНЫХ ЧАСТИЦ И АТОМНОГО ЯДРА»
1999, ТОМ 30, ВЫП. 4

УДК 939.1.01

TOPICS IN THE TRANSPORT THEORY OF QUARK-GLUON PLASMA

S. Mrówczyński

Soltan Institute for Nuclear Studies, ul. Hoża 69, PL - 00-681 Warsaw, Poland
and Institute of Physics, Pedagogical University,
ul. Konopnickiej 15, PL - 25-406 Kielce, Poland
E-mail: MROW@FUW.EDU.PL

«ФИЗИКА ЭЛЕМЕНТАРНЫХ ЧАСТИЦ И АТОМНОГО ЯДРА»
1999, ТОМ 30, ВЫП. 4

УДК 939.1.01

TOPICS IN THE TRANSPORT THEORY OF QUARK-GLUON PLASMA

S. Mrówczyński

Soltan Institute for Nuclear Studies, ul. Hoża 69, PL - 00-681 Warsaw, Poland
and Institute of Physics, Pedagogical University,
ul. Konopnickiej 15, PL - 25-406 Kielce, Poland
E-mail: MROW@FUW.EDU.PL

A few topics of the transport theory of quark-gluon plasma are reviewed. A derivation of the transport equations form the underlaying dynamical theory, is discussed within the ϕ^4 model. Peculiarities of the kinetic equations of quarks and gluons are considered, and the plasma (linear) response to the color field is studied. The chromoelectric tensor permeability is found and the plasma oscillations are discussed. Finally, the filamentation instability in the strongly anisotropic parton system from ultrarelativistic heavy-ion collisions is discussed in detail.

Рассмотрены некоторые избранные вопросы транспортной теории кварк-глюонной плазмы. Вывод формы транспортных уравнений, лежащих в основе динамической теории, обсуждается в рамках модели ϕ^4. Рассмотрены особенности кинетических уравнений кварков и глюонов и изучен плазменный (линейный) отклик цветных полей. Найден хромоэлектрический тензор проницаемости и обсуждаются плазменные осцилляции. В заключение детально обсуждаются нестабильности, связанные с нагревом сильно анизотропной системы, образующейся при соударениях тяжелых ионов.

1. INTRODUCTION

The quark-gluon plasma (QGP) is a macroscopic system of deconfined quarks and gluons. The very existence of QGP at a sufficiently large temperature and/or baryon density is basically an unavoidable consequence of the quantum chromodynamics (QCD), which is a dynamical theory of strong interactions (see, e.g., [1]). The plasma has been present in the early Universe and presumably can be found in the compact stellar objects. Of particular interest however is the generation of QGP in relativistic heavy-ion collisions, which has been actively studied theoretically and experimentally [2] for over ten years. The lifetime of the plasma produced, if indeed produced, in these collisions is not much longer than the characteristic time scale of parton processes*. Therefore, QGP can achieve,

*The word *parton* is used as a common name of quarks and gluons.

in the best case, only a quasi-equilibrium state and studies of the nonequilibrium phenomena are crucial to discriminate the characteristic features of QGP.

The transport or kinetic theory provides a natural framework to study systems out of thermodynamical equilibrium. Although the theory was initiated more than a century ago — Boltzmann derived his famous equation in 1872 — the theory is still under vital development. Application of Boltzmann's ideas to the systems, which are relativistic and of quantum nature, is faced with difficulties which have been overcome only partially till now. For a review see the monography [3]. In the case of the quark-gluon plasma specific difficulties appear due to the non-Abelian dynamics system. Nevertheless, the transport theory approach to QGP is in fast progress, and some interesting results have been already found.

The aim of this article is to review a few topics of the QGP transport theory. The first one is how to derive the transport equations of quarks and gluons. Since QCD is the underlying dynamical theory, these equations should be deduced from QCD. However, the kinetic theory of quarks and gluons has been successfully derived from QCD only in the mean-field or collisionless limit [4,5]. The derivation of the collision terms is still an open question. We discuss here the issue within the dynamical model which is much simpler than QCD. Namely, we consider the self interacting scalar fields with the quartic interaction term. Then, one can elucidate the essence of the derivation problem.

In the third chapter we present the transport equations of quarks and gluons obtained in the mean-field limit. The equations are supplemented by the collision terms which are justified on the phenomenological ground. We briefly discuss the peculiarities of the transport theory of quarks and gluons and then consider the locally colorless plasma*. The dynamical content of QCD enters here only through the cross sections of parton-parton interactions.

The characteristic features of QGP appear when the plasma is not locally colorless and consequently it interacts with the chromodynamic mean field. The plasma response to such a field is discussed in the fourth chapter, where the color conductivity and chromoelectric permeability tensors are found. We also analyse there the oscillations around the global thermodynamical equilibrium.

The parton momentum distribution is expected to be strongly anisotropic at the early stage of ultrarelativistic heavy-ion collisions. Then, the parton system can be unstable with respect to the specific plasma modes. In the fifth chapter we discuss in detail the mode which splits the parton system into the color current filaments parallel to the beam direction. We show why the fluctuation which

*We call the plasma *locally colorless* if the color four-current vanishes at each space-time point. It differs from the terminology used in the electron-ion plasma physics, where the plasma is called *locally neutral* if the electric charge (zero component of electromagnetic four-current) is everywhere zero.

initiates the filamentation can be very large and explain the physical mechanism responsible for the fluctuation growth. Then, the exponentially growing mode is found as a solution of the respective dispersion equation. The characteristic time of the instability development is estimated and finally, the possibility of observing the color filamentation in nucleus-nucleus collisions at RHIC and LHC is considered.

Presenting the QGP transport theory we try to avoid model dependent concepts but a very crucial assumption is adopted that the plasma is *perturbative*, i.e., the partons weakly interact with each other. As known, QGP becomes perturbative only at the temperatures much greater than the QCD scale parameter $\Lambda \cong 200$ MeV, see, e.g., [6]. However, one believes that many results obtained in the framework of the perturbative QCD can be extrapolated to the *nonperturbative* regime.

In the whole article we use the units where $c = k = \hbar = 1$. The metric tensor is diagonal with $g_{00} = -g_{11} = -g_{22} = -g_{33} = 1$.

2. DERIVATION OF THE TRANSPORT EQUATION IN ϕ^4 MODEL

The transport equations can be usually derived by means of simple heuristic arguments similar to those which were used by Boltzmann when he formulated the kinetic theory of gases. However, such arguments are insufficient when one studies a system of complicated dynamics as the quark-gluon plasma governed by QCD. Then, one has to refer to a formal scheme which allows one to derive the transport equation directly from the underlying quantum field theory. The formal scheme is also needed to specify the limits of the kinetic approach. Indeed, the derivation shows the assumptions and approximations which lead to the transport theory, and hence the domain of its applicability can be established.

Until now the transport equations of the QCD plasma have been successfully derived in the mean-field limit [4, 5] and the structure of these equations is well understood [4, 5, 7–10]. In particular, it has been shown that in the quasi-equilibrium these equations provide [5, 8] the so-called hard thermal loops [11]. The collisionless transport equations can be applied to the variety of problems. However, one needs the collision terms to discuss dissipative phenomena. In spite of some efforts [12–15], the general form of these terms in the transport equations of the quark-gluon plasma remains unknown. The QCD transport equations should also take into account the particle creation and annihilation which are entirely absent in the nonrelativistic atomic systems described by the Boltzmann equation. The particle production can occur due to the particle collisions or the presence of the strong fields as in the Schwinger mechanism [16]. The latter phenomenon has been actively studied in the context of the quark-gluon transport theory, see, e.g., [17–22]. However, one has had to refer to the simplifying assumption, as the (quasi-)homogeneity of the field, to get a tractable equations.

The so-called Schwinger–Keldysh [23, 24] formulation of the quantum field theory provides a very promising basis to derive the transport equation beyond the mean-field limit. Kadanoff and Baym [25] developed the technique for non-relativistic quantum systems which have been further generalized to relativistic ones [14, 26–35]. We mention here only the papers which provide a more or less systematic analysis of the collision terms.

The derivation of the complete QCD transport equations appears to be a very difficult task. In particular, the treatment of the massless fields such as gluons is troublesome. Except the well-known infrared divergences, which plague the perturbative expansion, there is a specific problem of nonequilibrium massless fields. The inhomogeneities in the system cause the off-mass-shell propagation of particles and then the perturbative analysis of the collision terms appears hardly tractable. More specifically, it appears very difficult, if possible at all, to express the field self-energy as the transition matrix element squared and consequently we loose the probabilistic character of the kinetic theory. The problem is absent for the massive fields when the system is assumed to be homogeneous at the inverse mass or Compton scale. This is a natural assumption within the transport theory which anyway deals with the quantities averaged over a certain scale which can be identified with the Compton one. We have developed [36] a systematic approach to the transport of massless fields, which allows one to treat these fields in a very similar manner as the massive ones. The basic idea is rather obvious. The fields which are massless in vacuum gain an effective mass in a medium due to the interaction. Therefore, the minimal scale at which the transport theory works is not an inverse bare mass, which is infinite for massless fields, but the inverse effective one. The starting point of the perturbative computation should be no longer free fields but the interacting ones. In physical terms, we have postulated existence of the massive quasi-particles and look for their transport equation. We have successfully applied the method to the massless scalar fields [36], but the generalization to QCD is far not straightforward due to the much reacher quasi-particle spectrum.

To demonstrate the characteristic features of the transport theory derivation we discuss in this chapter the simplest nontrivial model, i.e., the real massive fields with the Lagrangian density of the form

$$\mathcal{L}(x) = \frac{1}{2}\partial^{\mu}\phi(x)\partial_{\mu}\phi(x) - \frac{1}{2}m^2\phi^2(x) - \frac{g}{4!}\phi^4(x) \; . \tag{2.1}$$

The main steps of the derivation are the following. One defines the contour Green function with the time arguments on the contour in a complex time plane. This function, which is a key element of the Schwinger–Keldysh approach, satisfies the Dyson–Schwinger equation. Assuming the macroscopic quasi-homogeneity of the system, one performs the gradient expansion and the Wigner transformation. Then, the pair of Dyson–Schwinger equations is converted into the transport and

mass-shell equations both satisfied by the Wigner function. One further computes perturbatively the self-energy which provides the Vlasov and the collisional terms of the transport equation. Finally, one defines the distribution function of standard probabilistic interpretation and finds the transport equation satisfied by this function.

2.1. Green Functions. The contour Green function is defined as

$$i\Delta(x,y) \stackrel{\text{def}}{=} \langle \tilde{T}\phi(x)\phi(y)\rangle \ ,$$

where $\langle ....\rangle$ denotes the ensemble average at time t_0 (usually identified with $-\infty$); $\tilde{T}$ is the time ordering operation along the directed contour shown in Fig. 1. The parameter t_{max} is shifted to $+\infty$ in the calculations. The time arguments are complex with an infinitesimal positive or negative imaginary part, which locates them on the upper or on the lower branch of the contour. The ordering operation is defined as

$$\tilde{T}\phi(x)\phi(y) \stackrel{\text{def}}{=} \Theta(x_0,y_0)\phi(x)\phi(y) + \Theta(y_0,x_0)\phi(y)\phi(x) \ ,$$

where $\Theta(x_0,y_0)$ equals 1 if x_0 succeeds y_0 on the contour and equals 0 when x_0 precedes y_0.

If the field is expected to develop a finite expectation value, as it happens when the symmetry is spontaneously broken, the contribution $\langle\phi(x)\rangle\langle\phi(y)\rangle$ is subtracted from the right-hand side of the equation defining the Green function, see, e.g., [30, 31]. Then, one concentrates on the field fluctuations around the expectation values. Since $\langle\phi(x)\rangle$ is expected to vanish in the models defined by the Lagrangians (2.1), we neglect this contribution in the Green function definition.

We also use four other Green functions with real time arguments:

$$i\Delta^{>}(x,y) \stackrel{\text{def}}{=} \langle\phi(x)\phi(y)\rangle \ ,$$

$$i\Delta^{<}(x,y) \stackrel{\text{def}}{=} \langle\phi(y)\phi(x)\rangle \ ,$$

$$i\Delta^{c}(x,y) \stackrel{\text{def}}{=} \langle T^c\phi(x)\phi(y)\rangle \ ,$$

$$i\Delta^{a}(x,y) \stackrel{\text{def}}{=} \langle T^a\phi(x)\phi(y)\rangle \ ,$$

where $T^c(T^a)$ prescribes (anti-)chronological time ordering:

$$T^c\phi(x)\phi(y) \stackrel{\text{def}}{=} \Theta(x_0-y_0)\phi(x)\phi(y) + \Theta(y_0-x_0)\phi(y)\phi c(x) \ ,$$

$$T^a\phi(x)\phi(y) \stackrel{\text{def}}{=} \Theta(y_0-x_0)\phi(x)\phi(y) + \Theta(x_0-y_0)\phi(y)\phi(x) \ .$$

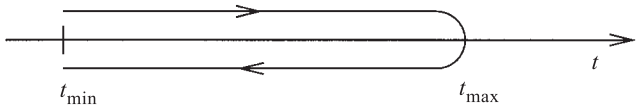

Fig. 1. The contour along the time axis for an evaluation of the operator expectation values

These functions are related to the contour Green functions in the following manner:

$$\Delta^c(x,y) \equiv \Delta(x,y) \text{ for } x_0,\ y_0 \text{ from the upper branch,}$$

$$\Delta^a(x,y) \equiv \Delta(x,y) \text{ for } x_0,\ y_0 \text{ from the lower branch,}$$

$$\Delta^>(x,y) \equiv \Delta(x,y) \text{ for } \begin{array}{ll} x_0 & \text{from the upper branch and} \\ y_0 & \text{from the lower one,} \end{array}$$

$$\Delta^<(x,y) \equiv \Delta(x,y) \text{ for } \begin{array}{ll} x_0 & \text{from the lower branch and} \\ y_0 & \text{from the upper one.} \end{array}$$

It appears convenient to introduce the retarded $(+)$ and advanced $(-)$ Green functions

$$\Delta^{\pm}(x,y) \stackrel{\text{def}}{=} \pm\Big(\Delta^>(x,y) - \Delta^<(x,y)\Big)\Theta(\pm x_0 \mp y_0)\ . \tag{2.2}$$

One easily finds several identities which directly follow from the definitions and relate the Green functions to each other.

$\Delta^c(x,y)$ describes the propagation of disturbance in which a single particle is added to the many-particle system in space-time point y and then is removed from it in a space-time point x. An antiparticle disturbance is propagated backward in time. The meaning of $\Delta^a(x,y)$ is analogous but particles are propagated backward in time; and antiparticles, forward. In the zero density limit $\Delta^c(x,y)$ coincides with the Feynman propagator.

The physical meaning of functions $\Delta^>(x,y)$ and $\Delta^<(x,y)$ is more transparent when one considers the Wigner transform defined as

$$\Delta^{\lessgtr}(X,p) \stackrel{\text{def}}{=} \int d^4u e^{ipu}\Delta^{\lessgtr}(X+\frac{1}{2}u, X-\frac{1}{2}u)\ . \tag{2.3}$$

Then, the free-field energy-momentum tensor averaged over ensemble can be expressed as

$$t_0^{\mu\nu}(X) \stackrel{\text{def}}{=} -\frac{1}{4}\langle\phi(x)\ \overset{\leftrightarrow}{\partial}{}^{\mu}\overset{\leftrightarrow}{\partial}{}^{\nu}\ \phi(x)\rangle = \int \frac{d^4p}{(2\pi)^4}p^\mu p^\nu i\Delta^<(X,p)\ .$$

One recognizes the standard form of the energy-momentum tensor in the kinetic theory with the function $i\Delta^<(X,p)$ giving the density of particles with four-momentum p in a space-time point X. Therefore, $i\Delta^<(X,p)$ can be treated as a quantum analog of the classical distribution function. Indeed, the function $i\Delta^<(X,p)$ is Hermitian. However, it is not positively definite and the probabilistic interpretation is only approximately valid. One should also observe that, in contrast to the classical distribution functions, $i\Delta^<(X,p)$ can be nonzero for the off-mass-shell four-momenta.

2.2. Equations of Motion. The Dyson–Schwinger equations satisfied by the contour Green function are

$$\left[\partial_x^2 + m^2\right]\Delta(x,y) = -\delta^{(4)}(x,y) + \int_C d^4x' \Pi(x,x')\Delta(x',y) \ , \qquad (2.4)$$

$$\left[\partial_y^2 + m^2\right]\Delta(x,y) = -\delta^{(4)}(x,y) + \int_C d^4x' \Delta(x,x')\Pi(x',y) \ , \qquad (2.5)$$

where $\Pi(x,y)$ is the self-energy; the integration over x_0' is performed on the contour and the function $\delta^{(4)}(x,y)$ is defined on the contour as

$$\delta^{(4)}(x,y) = \begin{cases} \delta^{(4)}(x-y) & \text{for} \quad x_0 \ , \ y_0 \ \text{from the upper branch,} \\ 0 & \text{for} \quad x_0 \ , \ y_0 \ \text{from the different branches,} \\ -\delta^{(4)}(x-y) & \text{for} \quad x_0 \ , \ y_0 \ \text{from the lower branch.} \end{cases}$$

Let us split the self-energy into three parts:

$$\Pi(x,y) = \Pi_\delta(x)\delta^{(4)}(x,y) + \Pi^>(x,y)\Theta(x_0,y_0) + \Pi^<(x,y)\Theta(y_0,x_0) \ .$$

As we shall see later, Π_δ provides a dominant contribution to the mean-field while $\Pi^\gtrless$ determines the collision terms of the transport equations.

With the help of the retarded and advanced Green functions (2.2) and the retarded and advanced self-energies defined in an analogous way, the equations (2.4) and (2.5) can be rewritten as

$$\begin{aligned} \left[\partial_x^2 + m^2 \right. &- \left. \Pi_\delta(x)\right]\Delta^\gtrless(x,y) \\ &= \int d^4x' \Big[\Pi^\gtrless(x,x')\Delta^-(x',y) + \Pi^+(x,x')\Delta^\gtrless(x',y)\Big] \ , \end{aligned} \qquad (2.6)$$

$$\begin{aligned} \left[\partial_y^2 + m^2 \right. &- \left. \Pi_\delta(y)\right]\Delta^\gtrless(x,y) \\ &= \int d^4x' \Big[\Delta^\gtrless(x,x')\Pi^-(x',y) + \Delta^+(x,x')\Pi^\gtrless(x',y)\Big] \ , \end{aligned} \qquad (2.7)$$

where all time integrations run from $-\infty$ to $+\infty$.

2.3. Towards the Transport Equation. The transport equations are derived under the assumption that the Green functions and the self-energies depend weakly on the sum of their arguments and that they are significantly different from zero only when the difference of their arguments is close to zero. For homogeneous systems, the dependence on $X = (x+y)/2$ drops out entirely due to the translational invariance and $\Delta(x,y)$ depends only on $u = x - y$. For weakly inhomogeneous, or quasi-homogeneous systems, the Green functions and self-energies are assumed to vary slowly with X. We additionally assume that the Green functions and self-energies are strongly *peaked* near $u = 0$, which means that the correlation length is *short*.

We will now convert the equations (2.6), (2.7) into the transport and mass-shell equations by implementing the above approximation and performing the Wigner transformation (2.3) for all Green functions and self-energies. This is done by means of the translation rules such as:

$$\begin{aligned}
\int d^4x' f(x,x')g(x',y) \quad &\longrightarrow \quad f(X,p)g(X,p) \\
&+ \quad \frac{i}{2}\left[\frac{\partial f(X,p)}{\partial p_\mu}\frac{\partial g(X,p)}{\partial X^\mu} - \frac{\partial f(X,p)}{\partial X^\mu}\frac{\partial g(X,p)}{\partial p_\mu}\right], \\
h(x)g(x,y) \quad &\longrightarrow \quad h(X)g(X,p) - \frac{i}{2}\frac{\partial h(X)}{\partial X^\mu}\frac{\partial g(X,p)}{\partial p_\mu}, \\
\partial^\mu_x f(x,y) \quad &\longrightarrow \quad (-ip^\mu + \frac{1}{2}\partial^\mu) f(X,p).
\end{aligned}$$

Here $\partial^\mu \equiv \frac{\partial}{\partial X_\mu}$ and the functions $f(x,y)$ and $g(x,y)$ satisfy the assumptions discussed above. The function $h(x)$ is assumed to be weakly dependent on x.

The kinetic theory deals only with averaged system characteristics. Thus, one usually assumes that the system is homogeneous on a scale of the Compton wave length of the quasi-particles. In other words, the characteristic length of inhomogeneities is assumed to be much larger than the inverse mass of quasi-particles. Therefore, we impose the condition

$$\left|\Delta^{\gtrless}(X,p)\right| \gg \left|\frac{1}{m^2}\partial^2\Delta^{\gtrless}(X,p)\right|, \tag{2.8}$$

which leads to the quasi-particle approximation. The requirement (2.8) renders the off-shell contributions to the Green functions $\Delta^{\gtrless}$ negligible. Thus, we deal with the quasi-particles having on-mass-shell momenta.

Applying the translation rules and the quasi-particle approximation to Eqs. (2.6), (2.7), we obtain

$$\left[p^\mu\partial_\mu \quad - \quad \frac{1}{2}\partial_\mu\Pi_\delta(X)\partial^\mu_p\right]\Delta^{\gtrless}(X,p)$$

$$
\begin{aligned}
&= \frac{i}{2}\Big(\Pi^{>}(X,p)\Delta^{<}(X,p) - \Pi^{<}(X,p)\Delta^{>}(X,p)\Big) \\
&- \frac{1}{4}\Big\{\Pi^{\gtrless}(X,p), \Delta^{+}(X,p) + \Delta^{-}(X,p)\Big\} \\
&- \frac{1}{4}\Big\{\Pi^{+}(X,p) + \Pi^{-}(X,p),\, \Delta^{\gtrless}(X,p)\Big\}\,, \qquad (2.9)
\end{aligned}
$$

$$
\begin{aligned}
\Big[-p^2 \;&+\; m^2 - \Pi_\delta(X)\Big]\Delta^{\gtrless}(X,p) \\
&= \frac{1}{2}\Big(\Pi^{\gtrless}(X,p)\big(\Delta^{+}(X,p) + \Delta^{-}(X,p)\big) \\
&+ \big(\Pi^{+}(X,p) + \Pi^{-}(X,p)\big)\Delta^{\gtrless}(X,p)\Big) \\
&+ \frac{i}{4}\Big\{\Pi^{>}(X,p),\, \Delta^{<}(X,p)\Big\} - \frac{i}{4}\Big\{\Pi^{<}(X,p),\, \Delta^{>}(X,p)\Big\}, \qquad (2.10)
\end{aligned}
$$

where we have introduced the Poisson-like bracket defined as

$$
\Big\{C(X,p),\, D(X,p)\Big\} \equiv \frac{\partial C(X,p)}{\partial p_\mu}\frac{\partial D(X,p)}{\partial X^\mu} - \frac{\partial C(X,p)}{\partial X^\mu}\frac{\partial D(X,p)}{\partial p_\mu}\,.
$$

One recognizes Eq. (2.9) as a transport equation, while Eq. (2.10), as a so-called mass-shell equation. We write down these equations in a more compact way:

$$
\begin{aligned}
\Big\{p^2 - m^2 + \Pi_\delta(X) \;&+\; \mathrm{Re}\Pi^{+}(X,p),\, \Delta^{\gtrless}(X,p)\Big\} \\
&= i\Big(\Pi^{>}(X,p)\Delta^{<}(X,p) - \Pi^{<}(X,p)\Delta^{>}(X,p)\Big) \\
&- \Big\{\Pi^{\gtrless}(X,p),\, \mathrm{Re}\Delta^{+}(X,p)\Big\}\,, \qquad (2.11)
\end{aligned}
$$

$$
\begin{aligned}
\Big[p^2 - m^2 \;&+\; \Pi_\delta(X) + \mathrm{Re}\Pi^{+}(X,p)\Big]\Delta^{\gtrless}(X,p) = -\Pi^{\gtrless}(X,p)\mathrm{Re}\Delta^{+}(X,p) \\
&- \frac{i}{4}\Big\{\Pi^{>}(X,p),\, \Delta^{<}(X,p)\Big\} + \frac{i}{4}\Big\{\Pi^{<}(X,p),\, \Delta^{>}(X,p)\Big\}\,. \qquad (2.12)
\end{aligned}
$$

The gradient terms in the right-hand sides of Eqs. (2.11), (2.12) are usually neglected [30, 31].

We introduce the spectral function A defined as

$$
A(x,y) \stackrel{\mathrm{def}}{=} \langle[\phi(x), \phi(y)]\rangle = i\Delta^{>}(x,y) - i\Delta^{<}(x,y)\,,
$$

where $[\phi(x), \phi(y)]$ denotes the field commutator. Due to the equal time commutation relations

$$
[\phi(t,\mathbf{x}), \phi(t,\mathbf{y})] = 0\,, \qquad [\dot{\phi}(t,\mathbf{x}), \phi(t,\mathbf{y})] = -i\delta^{(3)}(\mathbf{x}-\mathbf{y})\,,
$$

with the dot denoting the time derivative, the Wigner transformed spectral function satisfies the two identities

$$\int \frac{dp_0}{2\pi}\, A(X,p) = 0 \;, \qquad \int \frac{dp_0}{2\pi}\, p_0\, A(X,p) = 1 \;.$$

From the transport and mass-shell equations (2.11), (2.12) one immediately finds the equations satisfied by $A(X,p)$ which are

$$\Big\{p^2 - m^2 + \Pi_\delta(X) + \mathrm{Re}\Pi^+(X,p),\, A(X,p)\Big\} = 2\Big\{\mathrm{Im}\Pi^+(X,p),\, \mathrm{Re}\Delta^+(X,p)\Big\} \;, \tag{2.13}$$

$$\Big[p^2 - m^2 + \Pi_\delta(X) + \mathrm{Re}\Pi^+(X,p)\Big] A(X,p) = 2\,\mathrm{Im}\Pi^+(X,p)\,\mathrm{Re}\Delta^+(X,p) \;. \tag{2.14}$$

One solves the algebraic equation (2.14) as

$$A(X,p) = \frac{2\mathrm{Im}\Pi^+(X,p)}{\big(p^2 - m^2 + \Pi_\delta(X) + \mathrm{Re}\Pi^+(X,p)\big)^2 + \big(\mathrm{Im}\Pi^+(X,p)\big)^2} \;. \tag{2.15}$$

Then, it is shown that the function of the form (2.15) solves Eq. (2.13) as well. The spectral function of the free fields can be found as

$$A_0(X,p) = 2\pi\delta(p^2 - m^2)\big(\Theta(p_0) - \Theta(-p_0)\big) \;.$$

Since $\mathrm{Re}\Pi^+$ determines the quasi-particle effective mass and $\mathrm{Im}\Pi^+$ its width, the spectral function characterises the quasi-particle properties.

2.4. Perturbative Expansion. As discussed in, e.g., [28, 29, 37] the contour Green functions admit a perturbative expansion very similar to that known from the vacuum field theory with essentially the same Feynman rules. However, the time integrations do not run from $-\infty$ to $+\infty$, but along the contour shown in Fig. 1. The right turning point of the contour (t_{max}) must be above the largest time argument of the evaluated Green function. In practice, t_0 is shifted to $-\infty$ and t_{max} to $+\infty$. The second difference is the appearance of tadpoles, i.e., loops formed by single lines, which give zero contribution in the vacuum case. A tadpole corresponds to a Green function with two equal space-time arguments. Since the Green function $\Delta(x,y)$ is not well defined for $x = y$ we ascribe the function $-i\Delta^<(x,x)$ to each tadpole. The rest of Feynman rules can be taken from the textbook of Bjorken and Drell [38].

The lowest-order contribution to the self-energy, which is associated with the graph from Fig. 2, equals

$$\Pi(x,y) = -\frac{ig}{2}\delta^{(4)}(x,y)\Delta_0^<(x,x) \;,$$

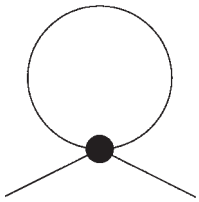

Fig. 2. The lowest-order diagram of the self-energy

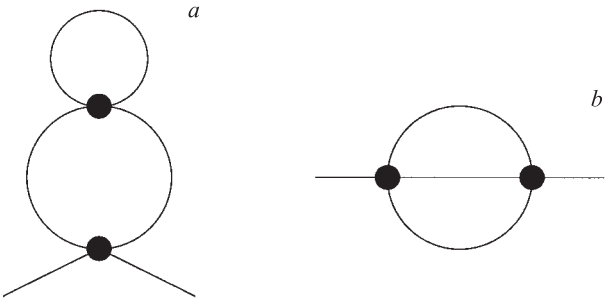

Fig. 3. The second-order diagrams of the self-energy

giving

$$\Pi_\delta(x) = -\frac{ig}{2}\Delta_0^<(x,x)\ , \tag{2.16}$$

and

$$\Pi^>(x,y) = \Pi^<(x,y) = 0\ .$$

The one-particle irreducible g^2 contributions to the self-energy are shown in Fig. 3. The contribution corresponding to the diagram 3a can be easily computed. However, it is pure real and the only effect of this contributions is a higher order modification of the mean-field term. Thus, we do not consider these diagrams but instead we analyse the contribution 3b which provides a qualitatively new effect. It gives the contour self-energy equal to

$$\Pi_c(x,y) = \frac{g^2}{6}\Delta_0(x,y)\Delta_0(y,x)\Delta_0(x,y)\ ,$$

and consequently

$$\Pi^{\gtrless}(x,y) = \frac{g^2}{6}\Delta_0^{\gtrless}(x,y)\Delta_0^{\lessgtr}(y,x)\Delta_0^{\gtrless}(x,y)\ . \tag{2.17}$$

2.5. Distribution Function and Transport Equation. The distribution function $f(X,p)$ is defined as

$$\Theta(p_0) i\Delta^<(X,p) = \Theta(p_0)\; A(X,p)\; f(X,p)\;,$$

where $A(X,p)$ is the spectral function (2.15). Then, one finds [36] that

$$i\Delta^>(X,p) = \Theta(p_0)\; A(X,p)\; \big(f(X,p)+1\big) - \Theta(-p_0)\; A(X,p)\; f(X,-p), \tag{2.18}$$

$$i\Delta^<(X,p) = \Theta(p_0)\; A(X,p)\; f(X,p) - \Theta(-p_0)\; A(X,p)\; \big(f(X,-p)+1\big). \tag{2.19}$$

There is a very important property of $\Delta^{\gtrless}$ expressed in the from (2.18), (2.19). Namely, if the Green functions $\Delta^{\gtrless}$ satisfy the transport equation (2.11) and the spectral function solves the equation (2.14), the mass-shell equation of $\Delta^{\gtrless}$, i.e., Eq. (2.12), is satisfied *automatically* in the 0-th order of the gradient expansion. Let us note that the quasi-particle dispersion relation is found as a solution of the equation

$$p^2 - m^2 + \Pi_\delta(X) + \mathrm{Re}\Pi^+(X,p) = 0\;. \tag{2.20}$$

The distribution function f satisfies the transport equation which can be obtained from Eq. (2.11) for $\Delta^>$ or $\Delta^<$. After using Eq. (2.13) one finds

$$\begin{aligned} A(X,p)\Big\{p^2 - m^2 \;&+\; \mathrm{Re}\Pi^+(X,p),\, f(X,p)\Big\} \\ &= iA(X,p)\Big(\Pi^>(X,p)\, f(X,p) - \Pi^<(X,p)\,\big(f(X,p)+1\big)\Big) \\ &+ if(X,p)\Big\{\Pi^>(X,p),\, \mathrm{Re}\Delta^+(X,p)\Big\} \\ &- i\big(f(X,p)+1\big)\Big\{\Pi^<(X,p),\, \mathrm{Re}\Delta^+(X,p)\Big\}\;, \end{aligned} \tag{2.21}$$

where $p_0 > 0$. We have also used here the following property of the Poisson-like brackets:

$$\big\{A,\, B\,C\big\} = \big\{A,\, B\big\}\,C + \big\{A,\, C\big\}\,B\;.$$

The left-hand side of Eq. (2.21) is a straightforward generalization of the drift term of the standard relativistic transport equation. Computing the Poisson-like bracket and imposing the mass-shell constraint one finds the familiar structure

$$\begin{aligned} \frac{1}{2}\Theta(p_0)\Big\{p^2 - m^2 \;&+\; \mathrm{Re}\Pi^+(X,p),\, f(X,p)\Big\} \\ &= E_p\Big(\frac{\partial}{\partial t} + \mathbf{v}\nabla\Big) f(X,p) - \nabla \mathrm{Re}\Pi^+(X,p)\cdot\nabla_p f(X,p)\;, \end{aligned}$$

where the velocity $\mathbf{v}$ equals $\partial E_p/\partial\mathbf{p}$ with the (positive) energy E_p being the solution of the dispersion equation (2.20).

Let us now analyse the right-hand side of Eq. (2.21). The collision terms are provided by the self-energies (2.17). Since the quasi-particles of interest are narrow ($m^2 + \mathrm{Re}\Pi^+ \gg \mathrm{Im}\Pi^+$), we take into account only those terms contributing to $\Pi^{\gtrless}$ which are nonzero for the on-mass-shell momenta. The other terms are negligibly small [36]. Then, the first term in r.h.s of the transport equation (2.21) is very similar to the standard collision term [3] of the Nordheim [39] (or Uehling–Uhlenbeck [40]) form. Indeed,

$$\begin{aligned} i\Big(\Pi^{>}(X,p)\, f(X,p) \quad &- \quad \Pi^{<}(X,p)\,\big(f(X,p)+1\big)\Big) \\ &= \quad \frac{g^2}{2}\int \frac{d^4k A_k^+}{(2\pi)^4}\,\frac{d^4q A_q^+}{(2\pi)^4}\,\frac{d^4r A_r^+}{(2\pi)^4}\,(2\pi)^4\delta^{(4)}(p+q-k-r) \\ &\times \quad \Big((f^p+1)(f^q+1)\,f^k\,f^r - f^p\,f^q(f^k+1)(f^r+1)\Big), \end{aligned}$$

where $A_k^+ \equiv \Theta(k_0)\; A(X,k)$ and $f^k \equiv f(X,k)$. The last two terms from r.h.s of Eq. (2.21), which are neglected in the usual transport equation, are discussed in [36].

3. TRANSPORT EQUATIONS OF QUARKS AND GLUONS

In this chapter we introduce the gauge dependent distribution functions of quarks and gluons. Then, we discuss the transport equations satisfied by these functions. Finally, a very useful notion of the locally colorless plasma is considered.

3.1. Distribution Functions. The (anti-)quark distribution function $Q(p,x)\big(\bar{Q}(p,x)\big)$ is a Hermitian $N_c \times N_c$ matrix in color space (for a $SU(N_c)$ color group) with p denoting the quark four-momentum and x the space-time coordinate [41–43]. The function transforms under local gauge transformations as

$$Q(p,x) \to U(x)Q(p,x)U^\dagger(x)\ . \tag{3.1}$$

The color indices are here and in most cases below suppressed.

The gluon distribution function [44] is a Hermitian $(N_c^2-1)\times(N_c^2-1)$ matrix [7] which transforms as

$$G(p,x) \to M(x)G(p,x)M^\dagger(x)\ , \tag{3.2}$$

where

$$M_{ab}(x) = \mathrm{Tr}\big[\tau_a U(x)\tau_b U^\dagger(x)\big],$$

with $\tau_a,\ a = 1,...,N_c^2-1$ being the $SU(N_c)$ group generators in the fundamental representation. One sees that, in contrast to the distribution functions known from

the physics of atomic gases, the distribution functions of quarks and gluons have no simple probabilistic interpretation due to the gauge dependence. This is, however, not surprising if one realizes that the question about the probability to find, let us say, a red quark in a phase-space cell centered around (p,x) is not physical since the color of a quark can be changed by means of a gauge transformation.

It follows from the transformation laws (3.1), (3.2) that the traces of the distribution functions are gauge independent, and consequently they can have a familiar probabilistic interpretation. Indeed, the probability to find a quark of arbitrary color in a cell (p,x) is of physical meaning since it is gauge independent. The quantities, which are color (gauge) independent like the baryon current b^μ or the energy momentum tensor $t^{\mu\nu}$, are entirely expressed through the traces of the distribution functions

$$\begin{aligned} b^\mu(x) &= \frac{1}{3}\int \frac{d^3p}{(2\pi)^3 E}\, p^\mu \Big[\mathrm{Tr}\big[Q(p,x)\big] - \mathrm{Tr}\big[\bar{Q}(p,x)\big]\Big]\,, \\ t^{\mu\nu}(x) &= \int \frac{d^3p}{(2\pi)^3 E}\, p^\mu p^\nu \Big[\mathrm{Tr}\big[Q(p,x)\big] + \mathrm{Tr}\big[\bar{Q}(p,x)\big] + \mathrm{Tr}\big[G(p,x)\big]\Big]\,, \end{aligned}$$

with E being the quark or gluon energy. Both quarks and gluons are assumed to be massless and their spin is treated as an internal degree of freedom. The spin structure of the distribution functions and the respective transport equations have been discussed in [9, 10].

The color current, which is a gauge dependent quantity, is expressed not only through the traces of the distribution functions but also through the functions themselves. In the $N_c \times N_c$ matrix notation the current reads

$$\begin{aligned} j^\mu(x) = -\frac{1}{2}g\int \frac{d^3p}{(2\pi)^3 E}\, p^\mu \Big[Q(p,x) - \bar{Q}(p,x) &- \frac{1}{N_c}\mathrm{Tr}\big[Q(p,x) - \bar{Q}(p,x)\big] \\ &+ 2i\tau_a f_{abc} G_{bc}(p,x)\Big]\,, \end{aligned} \tag{3.3}$$

where g is the QCD coupling constant and f_{abc} are the structure constants of the $SU(N_c)$ group. In the adjoint representation the color current (3.3) is

$$j^\mu_a(x) = -g\int \frac{d^3p}{(2\pi)^3 E}\, p^\mu \Big[\mathrm{Tr}\big[\tau_a\big(Q(p,x) - \bar{Q}(p,x)\big)\big] + i f_{abc} G_{bc}(p,x)\Big]\,,$$

where we have used the equality $\mathrm{Tr}(\tau_a\tau_b) = \frac{1}{2}\delta_{ab}$.

3.2. Transport Equations. The distribution functions of quarks and gluons satisfy the following set of transport equations [4, 7, 41–44]:

$$p^\mu D_\mu Q(p,x) + g p^\mu \frac{\partial}{\partial p_\nu}\frac{1}{2}\{F_{\mu\nu}(x), Q(p,x)\} = C[Q,\bar{Q},G]\,,$$

$$
\begin{aligned}
p^\mu D_\mu \bar{Q}(p,x) - g p^\mu \frac{\partial}{\partial p_\nu} \frac{1}{2} \{F_{\mu\nu}(x), \bar{Q}(p,x)\} &= \bar{C}[Q, \bar{Q}, G] \, , \\
p^\mu \mathcal{D}_\mu G(p,x) + g p^\mu \frac{\partial}{\partial p_\nu} \frac{1}{2} \{\mathcal{F}_{\mu\nu}(x), G(p,x)\} &= C_g[Q, \bar{Q}, G] \, , \qquad (3.4)
\end{aligned}
$$

where $\{..., ...\}$ denotes the anicommutator; D_μ and $\mathcal{D}_\mu$ are the covariant derivatives which act as

$$
D_\mu = \partial_\mu - ig[A_\mu(x), ...] \, , \qquad \mathcal{D}_\mu = \partial_\mu - ig[\mathcal{A}_\mu(x), ...] \, ,
$$

where A_μ and $\mathcal{A}_\mu$ are the mean-field four-potentials defined as

$$
A^\mu(x) = A^\mu_a(x) \tau_a \, , \qquad \mathcal{A}^\mu_{ab}(x) = -i f_{abc} A^\mu_c(x) \, .
$$

$F_{\mu\nu}$ and $\mathcal{F}_{\mu\nu}$ are the mean-field stress tensors with a color index structure analogous to that of the four-potentials. The mean-field is generated by the color current (3.3) and the respective equation is

$$
D_\mu F^{\mu\nu}(x) = j^\nu(x) \, . \qquad (3.5)
$$

C, $\bar{C}$ and C_g are the collision terms which vanish in the collisionless limit, i.e., when the plasma evolution is dominated by the mean-field effects*. As already mentioned, the collision terms of the QGP kinetic equations have not been systematically derived yet and their structure remains obscure. The situation simplifies in the case of the colorless plasma discussed in the next section. We note that the set of transport equations (3.4), (3.5) is covariant with respect to the gauge transformations (3.1), (3.2).

3.3. Colorless Plasma. Evolving towards thermodynamical equilibrium the system of quarks of gluons tends to neutralize color charges. It is expected [13] that after a short period of time the plasma becomes locally colorless, the color current and the mean-field $F^{\mu\nu}$ vanish. Then, the distribution functions of quarks and gluons are proportional to the unit matrices in the color space. Specifically,

$$
\begin{aligned}
Q_{ij}(p,x) &= \frac{1}{N_c} \delta_{ij} \, q(p,x) \, , \quad i,j = 1, ..., N_c \, , \\
\bar{Q}_{ij}(p,x) &= \frac{1}{N_c} \delta_{ij} \, \bar{q}(p,x) \, , \\
G_{ab}(p,x) &= \frac{1}{N_c^2 - 1} \delta_{ab} \, g(p,x) \, , \quad a,b = 1, ..., N_c^2 - 1 \, .
\end{aligned}
$$

As is seen, the distribution functions of the colorless plasma are gauge invariant.

*This occurs when the characteristic mean-field frequency is much greater than the parton collision frequency.

The transport equations of the colorless plasma are essentially simplified. Indeed, taking the trace of Eqs. (3.4) one finds

$$\begin{aligned} p^\mu \partial_\mu q(x,p) &= c[q,\bar{q},g] \,, \\ p^\mu \partial_\mu \bar{q}(x,p) &= \bar{c}[q,\bar{q},g] \,, \\ p^\mu \partial_\mu g(x,p) &= c_g[q,\bar{q},g] \,, \end{aligned} \tag{3.6}$$

where $c \equiv \mathrm{Tr}C$, $\bar{c} \equiv \mathrm{Tr}\bar{C}$ and $c_g \equiv \mathrm{Tr}C_g$. Because the trace of a commutator is zero, the covariant derivatives reduce to the normal ones in (3.6).

In the case of a colorless plasma the color charges can be treated as internal degrees of freedom of the quarks and gluons, and it is sufficient to operate with the color averaged quantities which are gauge independent. Then, one can imitate the dynamics of the colorless plasma with a nongauge field theory model such as ϕ^4. Then, the collision terms are of the Nordheim [39] (or Uehling–Uhlenbeck [40]) form as discussed in the previous chapter. Therefore, even not knowing the collision terms C, $\bar{C}$, and C_g, we expect that the respective terms of the colorless plasma c, $\bar{c}$, and c_g, which represent the binary collisions, are

$$\begin{aligned} c[q,\bar{q},g] = \int \frac{d^3p_2}{(2\pi)^3 E_2} \frac{d^3p_3}{(2\pi)^3 E_3} \frac{d^3p_4}{(2\pi)^3 E_4} \\ \Big[\quad \tfrac{1}{2} \quad \big[q_3 q_4 (1-q_1)(1-q_2) - q_1 q_2 (1-q_3)(1-q_4)\big] W_{qq\to qq}(p_3,p_4|p_1,p_2) \\ + \quad \big[q_3 \bar{q}_4 (1-q_1)(1-\bar{q}_2) - q_1 \bar{q}_2 (1-q_3)(1-\bar{q}_4)\big] W_{q\bar{q}\to q\bar{q}}(p_3,p_4|p_1,p_2) \\ + \quad \big[q_3 g_4 (1-q_1)(1+g_2) - q_1 g_2 (1-q_3)(1+g_4)\big] W_{qg\to qg}(p_3,p_4|p_1,p_2) \\ + \quad \big[g_3 g_4 (1-q_1)(1-\bar{q}_2) - -q_1 \bar{q}_2 (1+g_3)(1+g_4)\big] W_{q\bar{q}\to gg}(p_3,p_4|p_1,p_2) \Big] \end{aligned} \tag{3.7}$$

with the analogous expressions for $\bar{c}[\bar{q},q,g]$ and $c_g[g,q,\bar{q},]$. We have used here the abbreviations $q_1 \equiv q(x,p_1)$, $q_2 \equiv q(x,p_2)$, etc. Furthermore $p_1 \equiv p$. The coefficient $\frac{1}{2}$ in the first line of the r.h.s. of Eq. (3.7) is required to avoid the double counting of identical particles. The quantities like $W_{qg\to qg}(p_3,p_4|p_1,p_2)$, which correspond to the quark-gluon scattering, are equal to the square of the respective matrix element multiplied by the energy-momentum conserving δ function. We note that the collision terms have to satisfy the relations

$$\begin{aligned} \int \frac{d^3p}{(2\pi)^3 E} \Big[c[q,\bar{q},g] - \bar{c}[q,\bar{q},g] \Big] &= 0 \,, \\ \int \frac{d^3p}{(2\pi)^3 E} p^\mu \Big[c[q,\bar{q},g] + \bar{c}[q,\bar{q},g] + c_g[q,\bar{q},g] \Big] &= 0 \,, \end{aligned}$$

in order to be consistent with the baryon number and energy-momentum conservation.

In the variety of applications one uses the collision terms in the relaxation time approximation, i.e.,

$$\begin{aligned} c &= \nu p_\mu u^\mu(x)\Big(q^{eq}(p,x) - q(p,x)\Big) , \\ \bar{c} &= \bar{\nu} p_\mu u^\mu(x)\Big(\bar{q}^{eq}(p,x) - \bar{q}(p,x)\Big) , \\ c_g &= \nu_g p_\mu u^\mu(x)\Big(g^{eq}(p,x) - g(p,x)\Big) , \end{aligned} \tag{3.8}$$

where ν, $\bar{\nu}$, and ν_g are the collision frequencies and u^μ is the hydrodynamic four-velocity which defines the local rest frame of the quark-gluon system. The equilibrium distribution functions are

$$\begin{aligned} q^{eq}(p,x) &= \frac{2N_f N_c}{\exp\big(\beta^\mu(x)p_\mu - \beta(x)\mu(x)\big)+1} , \\ \bar{q}^{eq}(p,x) &= \frac{2N_f N_c}{\exp\big(\beta^\mu(x)p_\mu + \beta(x)\mu(x)\big)+1} , \\ g^{eq}(p,x) &= \frac{2(N_c^2-1)}{\exp\big(\beta^\mu(x)p_\mu\big)-1} , \end{aligned}$$

where $\beta^\mu(x) \equiv \beta(x)u^\mu(x)$, $\beta(x) \equiv T^{-1}(x)$; $T(x)$ and $\mu(x)$ are the local temperature and quark chemical potential, respectively; N_f is the number of quark flavours. Spin, flavour and color are treated here as internal degrees of freedom.

4. PLASMA COLOR RESPONSE

In this chapter we discuss how the plasma, which is colorless, homogeneous and stationary, responses to the color small fluctuations.

4.1. Linear Response Analysis. The distribution functions are assumed to be of the form

$$\begin{aligned} Q_{ij}(p,x) &= n(p)\delta_{ij} + \delta Q_{ij}(p,x) , \\ \bar{Q}_{ij}(p,x) &= \bar{n}(p)\delta_{ij} + \delta \bar{Q}_{ij}(p,x) , \\ G_{ab}(p,x) &= n_g(p)\delta_{ab} + \delta G_{ab}(p,x) , \end{aligned} \tag{4.1}$$

where the functions describing the deviation from the colorless state are assumed to be much smaller than the respective colorless functions. The same is assumed for the momentum gradients of these functions.

Substituting (4.1) in (3.3) one gets

$$\begin{aligned} j^\mu(x) = &- \frac{1}{2} g \int \frac{d^3p}{(2\pi)^3 E}\, p^\mu \Big[\delta Q(p,x) - \delta\bar{Q}(p,x) \\ &- \frac{1}{N_c} Tr\big[\delta Q(p,x) - \delta\bar{Q}(p,x)\big] + 2i\tau_a f_{abc}\delta G_{bc}(p,x)\Big] . \end{aligned} \tag{4.2}$$

As is seen, the current occurs due to the deviation of the system from the colorless state. When the system becomes neutral, there is no current and one expects that there is no mean field. Therefore, we linearize Eq. (3.5) with respect to the four potential to the form

$$\partial_\mu F^{\mu\nu}(x) = j^\nu(x)$$

with $F^{\mu\nu} = \partial^\mu A^\nu - \partial^\nu A^\mu$. It should be stressed here that the linearization procedure does not cancel all non-Abelian effects. The gluon-gluon coupling, which is of essentially non-Abelian character is included because the gluons contribute to the color current (4.2). Let us also observe that in the linearized theory the color current is conserved (due to antisymmetry of $F^{\mu\nu}$) i.e., $\partial_\mu j^\mu = 0$. Finally we note that, as shown in [5], the semiclassical QCD transport theory effectively incorporates the resummation over the so-called hard thermal loops [11].

Now we substitute the distribution functions (4.1) to the transport equations (3.4) with the collision terms (3.8). Linearizing the equations with respect to δQ, $\delta\bar{Q}$, and δG, one gets

$$\begin{aligned}
\Big(p^\mu\partial_\mu \;+\; \nu p_\mu u^\mu\Big)\delta Q(p,x) \qquad\qquad & (4.3)\\
= \; -gp^\mu F_{\mu\nu}(x)\frac{\partial n(p)}{\partial p_\nu} + \nu p_\mu u^\mu\big(n^{eq}(p) - n(p)\big)\,,&\\
\Big(p^\mu\partial_\mu \;+\; \bar{\nu} p_\mu u^\mu\Big)\delta\bar{Q}(p,x)&\\
= \; gp^\mu F_{\mu\nu}(x)\frac{\partial \bar{n}(p)}{\partial p_\nu} + \bar{\nu} p_\mu u^\mu\big(\bar{n}^{eq}(p) - \bar{n}(p)\big)\,,&\\
\Big(p^\mu\partial_\mu \;+\; \nu_g p_\mu u^\mu\Big)\delta G(p,x)&\\
= \; -gp^\mu \mathcal{F}_{\mu\nu}(x)\frac{\partial n_g(p)}{\partial p_\nu} + \nu_g p_\mu u^\mu\big(n_g^{eq}(p) - n_g(p)\big)\,.&
\end{aligned}$$

Performing the linearization one should remember that A^μ is of the order of δQ. Treating the chromodynamic field as an external one, Eqs. (4.3) are easily solved

$$\begin{aligned}
\delta Q(p,x) \;&=\; -g\int d^4x'\Delta_p(x-x') \qquad\qquad & (4.4)\\
&\times\; \Big[p^\mu F_{\mu\nu}(x')\frac{\partial n(p)}{\partial p_\nu} - \nu p_\mu u^\mu\big(n^{eq}(p) - n(p)\big)\Big]\,,&\\
\delta\bar{Q}(p,x) \;&=\; g\int d^4x'\Delta_p(x-x')&\\
&\times\; \Big[p^\mu F_{\mu\nu}(x')\frac{\partial \bar{n}(p)}{\partial p_\nu} + \bar{\nu} p_\mu u^\mu\big(\bar{n}^{eq}(p) - \bar{n}(p)\big)\Big]\,,&
\end{aligned}$$

$$\begin{aligned}\delta G(p,x) &= -g\int d^4x'\Delta_p(x-x') \\ &\times \left[p^\mu \mathcal{F}_{\mu\nu}(x')\frac{\partial n_g(p)}{\partial p_\nu} - \nu_g p_\mu u^\mu\big(n_g^{eq}(p)-n_g(p)\big)\right],\end{aligned}$$

where $\Delta_p(x)$ is the Green function of the kinetic operator with the collision term in the relaxation time approximation,

$$\Delta_p(x) = E^{-1}\Theta(t)\, e^{-\nu' t}\,\delta^{(3)}(\mathbf{x}-\mathbf{v}t)\,,$$

with t being the zero component of x, $x^\mu \equiv (t,\mathbf{x})$, $\mathbf{v}\equiv \mathbf{p}/E$ and $\nu' \equiv \nu p^\mu u_\mu$; in the plasma rest frame $\nu' = \nu$.

Substituting the solutions (4.4) in Eq.(4.2) and performing the Fourier transformation with respect to x variable we get

$$j^\mu(k) = \sigma^{\mu\rho\lambda}(k)F_{\rho\lambda}(k) \tag{4.5}$$

with the color conductivity tensor expressed as

$$\begin{aligned}\sigma^{\mu\rho\lambda}(k) &= i\frac{g^2}{2}\int\frac{d^3p}{(2\pi)^3E}\Big[\frac{p^\mu p^\rho}{p^\sigma(k_\sigma+i\nu u_\sigma)}\frac{\partial n(p)}{\partial p_\lambda} \\ &+ \frac{p^\mu p^\rho}{p^\sigma(k_\sigma+i\bar\nu u_\sigma)}\frac{\partial \bar n(p)}{\partial p_\lambda} + \frac{2N_c p^\mu p^\rho}{p^\sigma(k_\sigma+i\nu_g u_\sigma)}\frac{\partial n_g(p)}{\partial p_\lambda}\Big]\,.\end{aligned} \tag{4.6}$$

If the plasma colorless state is isotropic, which is the case of the global equilibrium, one finds that $\sigma^{\mu\rho\lambda}(k) = \sigma^{\mu\rho}(k)u^\lambda$ and Eq. (4.5) gets more familiar form of the Ohm law, which in the plasma rest frame reads

$$j^\alpha(k) = \sigma^{\alpha\beta}(k)E^\beta(k)\,,$$

where the indices $\alpha,\beta,\gamma = 1,2,3$ label the space axes and $E^\alpha(k)$ is the α component of the chromoelectric vector. The conductivity tensor describes the response of the QGP to the chromodynamic field. Within the approximation used here it is a color scalar (no color indices) or equivalently is proportional to the unit matrix in the color space. In the next sections we will extract the information about QGP contained in $\sigma^{\mu\rho\lambda}(k)$.

4.2. Chromoelectric Permeability. Let us introduce, as in the electrodynamics, the polarization vector $\mathbf{P}(x)$ defined as

$$\mathrm{div}\mathbf{P}(x) = -\rho(x)\,,\quad \frac{\partial}{\partial t}\mathbf{P}(x) = \mathbf{j}(x)\,, \tag{4.7}$$

where ρ and $\mathbf{j}$ are the time-like and space-like components, respectively, of the color induced four-current, $j^\mu = (\rho,\mathbf{j})$. The definition (4.7) is self-consistent,

only when the color current is conserved, not covariantly conserved. This is just the case of the linear response approach. Further, we define the chromoelectric induction vector $\mathbf{D}(x)$,

$$\mathbf{D}(x) = \mathbf{E}(x) + \mathbf{P}(x) \tag{4.8}$$

and the chromoelectric permeability tensor, which relates the Fourier transformed **D** and **E** fields,

$$D^{\alpha}(k) = \epsilon^{\alpha\beta}(k) E^{\beta}(k) \; , \tag{4.9}$$

where $\alpha, \beta = 1, 2, 3$. Since the conductivity tensor (4.6) is a color scalar the permeability tensor is a color scalar as well.

Using the definitions (4.7), (4.8), (4.9) one easily finds that

$$\epsilon^{\alpha\beta}(k) = \delta^{\alpha\beta} - \frac{i}{\omega}\sigma^{\alpha 0\beta}(k) - \frac{i}{\omega^2}\Big[k^{\gamma}\sigma^{\alpha\beta\gamma}(k) - k^{\gamma}\sigma^{\alpha\gamma\beta}(k)\Big] \tag{4.10}$$

with $\sigma^{\alpha\gamma\beta}(k)$ given by Eq.(4.6); ω is the time-like component of the wave four-vector, $k^{\mu} \equiv (\omega, \mathbf{k})$. For the isotropic plasma the two last terms in Eq. (4.10) vanish. Substituting the conductivity tensor (4.6) into Eq. (4.10) we get the permeability tensor in the plasma rest frame

$$\begin{aligned} \epsilon^{\alpha\beta}(k) = \delta^{\alpha\beta} \quad &+ \quad \frac{g^2}{2\omega}\int \frac{d^3p}{(2\pi)^3}\Big[\frac{v^{\alpha}}{\omega - \mathbf{kv} + i\nu}\frac{\partial n(p)}{\partial p_{\gamma}} \\ &+ \quad \frac{v^{\alpha}}{\omega - \mathbf{kv} + i\bar{\nu}}\frac{\partial \bar{n}(p)}{\partial p_{\gamma}} \\ &+ \quad 2N_c\frac{v^{\alpha}}{\omega - \mathbf{kv} + i\nu_g}\frac{\partial n_g(p)}{\partial p_{\gamma}}\Big]\Big[\Big(1 - \frac{\mathbf{kv}}{\omega}\Big)\delta^{\gamma\beta} + \frac{k^{\gamma}v^{\beta}}{\omega}\Big] \; . \end{aligned} \tag{4.11}$$

In the case of the isotropic plasma the permeability tensor can be expressed as

$$\epsilon^{\alpha\beta}(k) = \epsilon_T(k)\Big(\delta^{\alpha\beta} - k^{\alpha}k^{\beta}/\mathbf{k}^2\Big) + \epsilon_L(k)\; k^{\alpha}k^{\beta}/\mathbf{k}^2$$

with the longitudinal and transversal permeability functions equal to

$$\begin{aligned} \epsilon_L(k) = 1 \quad &+ \quad \frac{g^2}{2\omega\mathbf{k}^2}\int \frac{d^3p}{(2\pi)^3}\Big[\frac{\mathbf{kv}\,k^{\gamma}}{\omega - \mathbf{kv} + i\nu}\frac{\partial n(p)}{\partial p_{\gamma}} \\ &+ \quad \frac{\mathbf{kv}\,k^{\gamma}}{\omega - \mathbf{kv} + i\bar{\nu}}\frac{\partial \bar{n}(p)}{\partial p_{\gamma}} + \frac{\mathbf{kv}\,k^{\gamma}}{\omega - \mathbf{kv} + i\nu_g}\frac{\partial n_g(p)}{\partial p_{\gamma}}\Big] \end{aligned} \tag{4.12}$$

$$\begin{aligned} \epsilon_T(k) = 1 \quad &+ \quad \frac{g^2}{2\omega}\int \frac{d^3p}{(2\pi)^3}\Big[\frac{1}{\omega - \mathbf{kv} + i\nu}\frac{\partial n(p)}{\partial p_{\gamma}} \\ &+ \quad \frac{1}{\omega - \mathbf{kv} + i\bar{\nu}}\frac{\partial \bar{n}(p)}{\partial p_{\gamma}} + \frac{1}{\omega - \mathbf{kv} + i\nu_g}\frac{\partial n_g(p)}{\partial p_{\gamma}}\Big]\Big[v^{\gamma} - \frac{\mathbf{kv}\,k^{\gamma}}{\mathbf{k}^2}\Big] \; . \end{aligned} \tag{4.13}$$

Because the QCD equations within the linear response approach coincide (up to the trivial matrix structure) with those of the electrodynamics, the dispersion relations of the plasma oscillations, or of plasmons, are those of the electrodynamics and they read [45,46]

$$\det \mid \mathbf{k}^2\delta^{\alpha\beta} - k^\alpha k^\beta - \omega^2\epsilon^{\alpha\beta}(k) \mid = 0 \ . \tag{4.14}$$

The relation (4.14) gets simpler form for the isotropic plasma. Namely,

$$\epsilon_L(k) = 0 \ , \quad \epsilon_T(k) = \mathbf{k}^2/\omega^2 \ . \tag{4.15}$$

The dispersion relations determine the plasma waves which can be propagated in the medium. Specifically, the plane wave with $\omega(\mathbf{k})$, which satisfies the dispersion equation (4.14), automatically solves the sourceless Maxwell equations in a medium. Using the 'quantum' language, the dispersion equation gives the relation between the energy and momentum of the quasi-particle excitations. In the case of plasma these are the transverse and longitudinal plasmons.

There are three classes of the solutions of Eq. (4.14). Those with pure real ω are stable — the wave amplitude is constant in time. If the imaginary part of frequency is negative, the oscillations are damped — the amplitude decreases in time. Of particular interest are the solutions with the positive Imω corresponding to the so-called plasma instabilities — the oscillations with the amplitude exponentially growing in time.

The permeability tensor in the static limit ($\omega \to 0$) provides the information about the plasma response to constant fields. Computing $\epsilon_L(\omega = 0, \mathbf{k})$ for the equilibrium collisionless plasma one finds

$$\epsilon_L(\omega = 0, \mathbf{k}) = 1 + \frac{m_D^2}{\mathbf{k}^2} \ ,$$

where m_D is the Debye mass which for the baryonless plasma of massless quarks and gluons equals

$$m_D^2 = \frac{g^2T^2(N_f + 2N_c)}{6} \ . \tag{4.16}$$

The chromoelectric potential of the static point-like source embedded in the plasma, which equals [46,47]

$$A_0(\mathbf{x}) = \frac{g}{4\pi \mid \mathbf{x} \mid} \exp(-m_D \mid \mathbf{x} \mid) \ ,$$

is screened at the distance $1/m_D$.

Since the parton density is $\sim T^3$, one finds from Eq. (4.16) that the number of partons in the Debye sphere (the sphere of the radius equal to the screening length) is $\sim 1/g^3$. It is much greater than unity if the plasma is *perturbative*,

i.e., when $1/g \gg 1$. A large parton number in the Debye sphere justifies, in particular, the use of the mean-field to describe QGP. Let us also mention that the ultrarelativistic *perturbative* plasma is automatically *ideal*, i.e., the average parton interaction energy, which is $\sim g^2/\langle r\rangle$, with $\langle r\rangle \sim T^{-1}$ being the average interparticle distance, is much smaller than the parton thermal energy which equals $\sim T$. This is not the case for the nonrelativistic electron plasma. Then, the screening length is (see, e.g., [46, 47])

$$m_D^2 = e^2 \frac{n_e}{T} ,$$

with n_e being the electron density*, which is independent of the temperature. As is seen, the smallness of the coupling constant does not guarantee that the nonrelativistic plasma is ideal. This occurs when the number of electrons in the Debye sphere is large, i.e., when $T^{3/2} \gg e^3 n_e^{1/2}$.

4.3. Oscillations Around the Global Equilibrium. Substituting the equilibrium distribution functions, Fermi–Dirac for quarks and Bose–Einstein for gluons, into Eqs. (4.13) and (4.14) one finds the permeability functions ϵ_L and ϵ_T, which for the collisionless ($\nu = \bar{\nu} = \nu_g = 0$) and baryonless ($\mu = 0$) plasma of massless partons can be computed analytically as

$$\epsilon_L = 1 + \frac{3\omega_0^2}{k^2}\left[1 - \frac{\omega}{2k}\Big[\ln \mid \frac{k+\omega}{k-\omega} \mid -i\pi\Theta(k-\omega)\Big]\right] , \tag{4.17}$$

$$\epsilon_T = 1 - \frac{3\omega_0^2}{2k^2}\left[1 - \Big(\frac{\omega}{2k} - \frac{k}{2\omega}\Big)\Big[\ln \mid \frac{k+\omega}{k-\omega} \mid -i\pi\Theta(k-\omega)\Big]\right] , \tag{4.18}$$

where $k \equiv \mid \mathbf{k} \mid$ and ω_0 is the plasma frequency equal to

$$\omega_0^2 = \frac{g^2 T^2 (N_f + 2N_c)}{18} . \tag{4.19}$$

One sees that for $\omega > k$ the dielectric functions (4.17), (4.18) are purely real, i.e., there are no dissipative processes.

Substituting (4.17), (4.18) into (4.15) one finds the dispersion relation of the longitudinal mode (the chromoelectric field parallel to the wave vector)

$$\omega^2 = \begin{cases} \omega_0^2 + \frac{3}{5}k^2 , & \text{for} \quad \omega_0 \gg k \\ k^2\Big(1 + 4\exp(-2 - 2k^2/3\omega_0^2)\Big) , & \text{for} \quad \omega_0 \ll k \end{cases}$$

*We use the units, where the fine structure constant $\alpha = e^2/4\pi$. In the Gauss units, which are traditionally used in the electron-ion plasma physics, $\alpha = e^2$.

and

$$\omega^2 = \begin{cases} \omega_0^2 + \frac{6}{5}k^2 \,, & \text{for} \quad \omega_0 \gg k \\ \frac{3}{2}\omega_0^2 + k^2 \,, & \text{for} \quad \omega_0 \ll k \end{cases}$$

for the transverse one (the chromoelectric field perpendicular to the wave vector). Because the longitudinal and transverse oscillations are time-like ($\omega^2 > k^2$), the phase velocity of the waves is greater than the velocity of light. For this reason the Landau damping is absent. As known, the Landau damping is due to the collisionless energy transfer from the wave to the plasma particles, the velocity of which is equal to the wave phase velocity [47].

The oscillations of the collisionless QGP around global equilibrium have been studied by means of the transport theory in several papers [7, 48, 51–53]. The problem has been also discussed in [49, 50] using a specific variant of the QGP theory with the classical color [41, 54]. In the above presentation we have followed [7]. The dispersion relations given above agree with those found in the finite-temperature QCD within the one-loop approximation, see, e.g., [6, 55–57].

Let us now consider the dielectric function with nonzero equilibration rates. As previously, the partons are massless and the plasma is baryonless which imposes $\nu = \bar{\nu}$. Then, one easily evaluates the integrals (4.13) and (4.14) for $\omega \gg k$, $\omega \gg \nu$ and $\omega \gg \nu_g$. The results read [7]:

$$\omega^2 = \omega_0^2 - \zeta^2 + \frac{3}{4}\phi^2 + \frac{3}{5}k^2 \,, \qquad \gamma = \frac{1}{2}\phi$$

for the longitudinal mode and

$$\omega^2 = \omega_0^2 - \zeta^2 + \frac{3}{4}\phi^2 + \frac{6}{5}k^2 \,, \qquad \gamma = \frac{1}{2}\phi \,,$$

for the transverse one; ω and γ denote the real and imaginary part, respectively, of the complex frequency; ϕ and ζ are parameters related to the equilibration rates,

$$\begin{aligned} \phi &= \nu \frac{N_f}{N_f + 2N_c} + \nu_g \frac{2N_c}{N_f + 2N_c} \,, \\ \zeta^2 &= \nu^2 \frac{N_f}{N_f + 2N_c} + \nu_g^2 \frac{2N_c}{N_f + 2N_c} \,. \end{aligned} \tag{4.20}$$

One sees that, when compared with the collisionless plasma, the frequency of the oscillations is smaller and the oscillations are damped. To find the numerical value of the damping rate — the plasma oscillation decrement γ — the equilibration rates (ν and ν_g) have to be estimated.

If ν or ν_g is identified with the mean free flight time controlled by the binary collisions, the equilibration rate is of the order of $g^4 \ln 1/g$. However, in the relativistic plasma there is another damping mechanism which is the plasmon

decay into quark-antiquark or gluon-gluon pair. It is easy to observe that, even in the limit of massless quarks, the decay into gluons is much more probable than that into quarks [7,57]. Let us consider the decay of plasmon of zero momentum. The phase-space volume of the decay final state is proportional to

$$\Big(1 \mp n^{eq}(\omega_0/2)\Big)^2 , \tag{4.21}$$

where the upper sign refers to quarks while the lower one to gluons. Since the plasma frequency (4.19) is much smaller than the temperature in the perturbative plasma, the factor (4.21) can be expanded as

$$\begin{aligned} \Big(1 - n^{eq}(\omega_0/2)\Big)^2 &\cong 1/4 + \omega_0/8T , \\ \Big(1 + n^{eq}(\omega_0/2)\Big)^2 &\cong 4T^2/\omega_0^2 . \end{aligned}$$

One sees that the decay into gluons is more probable than that into quarks by a factor of order g^{-2} [57].

Using the standard rules of finite-temperature field theory, one easily finds (see, e.g., [7]) the width of the zero-momentum plasmon due to the decay into gluons

$$\Gamma_d = \frac{g^2 N_c}{2^4 3\pi}\,\omega_0 \Big(1 + n^{eq}(\omega_0/2)\Big)^2 \cong \frac{g N_c T}{2^{3/2}\pi (N_f + 2N_c)^{1/2}} ,$$

which is the same for longitudinal and transverse plasmons. However, Γ_d cannot be identified with the plasmon equilibration rate Γ, because the plasmon decays are partially compensated by the plasmon formation processes. As shown in [58], see also [57], the formation rate Γ_f is related to Γ_d as

$$\Gamma_f = \exp(-\omega_0/T)\Gamma_d \cong (1 - \omega_0/T)\Gamma_d .$$

Since the equilibration rate of the plasmon $\Gamma = \Gamma_d - \Gamma_f$ [58], one finds [57]

$$\Gamma \cong \frac{g^2 N_c T}{12\pi} . \tag{4.22}$$

We note that Γ_d and Γ_f are of the order of g, while Γ is of the order of g^2. Since there is a preferred reference frame — the rest frame of the thermostat — the plasmon decay width is not a Lorentz scalar. Therefore, the result (4.22) is valid only for the zero-momentum or approximately long-wave plasmons.

Substituting ν_g equal (4.22) and $\nu = 0$ into Eq. (4.20), one estimates the decrement of the oscillation damping as

$$\gamma \cong \frac{g^2}{12\pi}\,\frac{N_c^2}{N_f + 2N_c}\,T . \tag{4.23}$$

Although $\nu = 0$ the damping rate depends on the number of quark flavours. This seems to be in agreement with the physical intuition. When the number of quark flavours is increased the inertia of the system is also increased, and consequently the time needed to damp the oscillations is longer. However Eq. (4.23) disagrees (by a factor of $2N_c/(N_f + 2N_c)$) with the result from [57], where γ equals (4.22). Unfortunately, the discrepancy cannot be resolved within the relaxation time approximation and a more elaborated analysis is needed.

5. FILAMENTATION INSTABILITY

In the near future the nucleus-nucleus collisions will be studied experimentally at the accelerators of a new generation: Relativistic Heavy-Ion Collider (RHIC) at Brookhaven and Large Hadron Collider (LHC) at CERN. The collision energy will be larger by one or two orders of magnitude than that one of the currently operating machines. A copious production of partons, mainly gluons, due to hard and semihard processes is expected in the heavy-ion collisions at this new energy domain [59, 60]. Thus, one deals with the many-parton system at the early stage of the collision. The system is on average locally colorless but random fluctuations can break the neutrality. Since the system is initially far from equilibrium, specific color fluctuations can exponentially grow in time and then noticeably influence the system evolution. While the very existence of such instabilities, similar to those which are known from the electron-ion plasma, see, e.g., [61], is fairly obvious and was commented upon long time ago [62], it is far less trivial to find those instabilities which are relevant for the parton system produced in ultrarelativistic heavy-ion collisions.

A system of two interpenetrating beams of nucleons [63, 64] or partons [65–69] was argued to be unstable with respect to the so-called filamentation or Weibel instability [70]. However, such a system appears to be rather unrealistic from the experimental point of view. Then, we have argued [71–73] that the filamentation can occur under weaker conditions which are very probable for heavy-ion collisions at RHIC and LHC. Instead of the two streams of partons, it appears sufficient to assume a strongly anisotropic momentum distribution. We systematically review here the whole problem.

5.1. Fluctuation Spectrum. We start with the discussion on how the unstable modes are initiated. Specifically, we show that the fluctuations, which act as seeds of the filamentation, are *large*, much larger than in the equilibrium plasma. Since the system of interest is far from the equilibrium, the fluctuations are not determined by the chromodielectric permeability tensor discussed in the previous section. The fluctuation-dissipation theorem does not hold in such a case. Thus, we derive the color current correlation function which provides the fluctuation spectrum.

QGP is assumed to be on average locally colorless, homogeneous and stationary. Therefore, the distribution functions averaged over ensemble are of the form

$$\langle Q_{ij}(t,\mathbf{x},\mathbf{p})\rangle = \delta^{ij} n(\mathbf{p}) \ , \qquad \langle \bar{Q}_{ij}(t,\mathbf{x},\mathbf{p})\rangle = \delta^{ij}\bar{n}(\mathbf{p}) \ ,$$
$$\langle G_{ab}(t,\mathbf{x},\mathbf{p})\rangle = \delta^{ab} n_g(\mathbf{p}) \ ,$$

which give the zero average color current.

We study the fluctuations of the color current generalizing a well-known approach to the fluctuating electric current [61]. For a system of noninteracting quarks and gluons we have derived (in the classical limit) the following expression of the current correlation tensor

$$\begin{aligned} M^{\mu\nu}_{ab}(t,\mathbf{x}) &\stackrel{\text{def}}{=} \langle j^{\mu}_a(t_1,\mathbf{x}_1) j^{\nu}_b(t_2,\mathbf{x}_2)\rangle \\ &= \frac{1}{8}\, g^2\, \delta^{ab} \int \frac{d^3p}{(2\pi)^3}\, \frac{p^\mu p^\nu}{E^2}\, f(\mathbf{p})\, \delta^{(3)}(\mathbf{x}-\mathbf{v}t) \ , \end{aligned} \tag{5.1}$$

where the effective parton distribution function $f(\mathbf{p})$ equals $n(\mathbf{p}) + \bar{n}(\mathbf{p}) + 2N_c n_g(\mathbf{p})$ and $(t,\mathbf{x}) \equiv (t_2 - t_1, \mathbf{x}_2 - \mathbf{x}_1)$. Due to the average space-time homogeneity the correlation tensor depends only on the difference $(t_2 - t_1, \mathbf{x}_2 - \mathbf{x}_1)$. The physical meaning of the formula (5.1) is transparent. The space-time points $(t_1,\mathbf{x}_1)$ and $(t_2,\mathbf{x}_2)$ are correlated in the system of noninteracting particles if the particles fly from $(t_1,\mathbf{x}_1)$ to $(t_2,\mathbf{x}_2)$. For this reason the delta $\delta^{(3)}(\mathbf{x}-\mathbf{v}t)$ is present in the formula (5.1). The momentum integral of the distribution function simply represents the summation over particles. The fluctuation spectrum is found as a Fourier transform of the tensor (5.1), i.e.,

$$M^{\mu\nu}_{ab}(\omega,\mathbf{k}) = \frac{1}{8}\, g^2\, \delta^{ab} \int \frac{d^3p}{(2\pi)^3}\, \frac{p^\mu p^\nu}{E^2}\, f(\mathbf{p})\, 2\pi\delta(\omega - \mathbf{k}\mathbf{v}) \ . \tag{5.2}$$

When the system is in equilibrium the fluctuations are given, according to the fluctuation-dissipation theorem, by the respective response function. For $f(\mathbf{p})$ being the classical equilibrium distribution function one indeed finds the standard fluctuation-dissipation relation [61] valid in the g^2order. For example,

$$M^{00}_{ab}(\omega,\mathbf{k}) = \delta^{ab} \frac{\mathbf{k}^2}{2\pi}\, \frac{T}{\omega}\, \mathrm{Im}\epsilon_L(\omega,\mathbf{k}) \ ,$$

where T is the temperature and ϵ_L represents the longitudinal part of the chromodielectric tensor (4.13).

5.2. Parton Distributions. We model the parton momentum distribution at the early stage of ultrarelativistic heavy-ion collision by two functions:

$$f(\mathbf{p}) = \frac{1}{2Y}\Theta(Y-y)\Theta(Y+y)\, h(p_\perp)\, \frac{1}{p_\perp \,\mathrm{ch}y} \ , \tag{5.3}$$

and

$$f(\mathbf{p}) = \frac{1}{2\mathcal{P}}\Theta(\mathcal{P} - p_\parallel)\Theta(\mathcal{P} + p_\parallel)\; h(p_\perp)\;, \tag{5.4}$$

where y, $p_\parallel$, and $p_\perp$ denote the parton rapidity, the longitudinal, and transverse momenta, respectively. The parton momentum distribution (5.3) corresponds to the rapidity distribution which is flat in the interval $(-Y, Y)$. The distribution (5.4) is flat for the longitudinal momentum $-\mathcal{P} < p_\parallel < \mathcal{P}$. We do not specify the transverse momentum distribution $h(p_\perp)$, which is assumed to be of the same shape for quarks and gluons, because it is sufficient for our considerations to demand that the distributions (5.3), (5.4) are strongly elongated along the $z-$axis, i.e., $e^Y \gg 1$ and $\mathcal{P} \gg \langle p_\perp \rangle$.

The QCD-based computations, see, e.g., [59,60], show that the rapidity distribution of partons produced at the early stage of heavy-ion collisions is essentially Gaussian with the width of about one to two units. When the distribution (5.3) simulates the Gaussian one, Y does not measure the size of the 'plateau' but rather the range over which the partons are spread. If one takes the Gaussian distribution of the variance σ and the distribution (5.3) of the same variance, then $Y = \sqrt{3}\,\sigma$.

As already mentioned, the parton system described by the distribution functions (5.3), (5.4) is assumed to be homogeneous and stationary. Applicability of this assumption is very limited because there is a correlation between the parton longitudinal momentum and its position, i.e., partons with very different momenta will find themselves in different regions of space shortly after the collision. However, one should remember that we consider the parton system at a very early stage of the collision, soon after the Lorentz contracted ultrarelativistic nuclei traverse each other. At this stage partons are most copiously produced but do not have enough time to escape from each other. Thus, the assumption of homogeneity holds for the space-time domain of the longitudinal size, say, $2 - 3$ fm and life time $2 - 3$ fm$/c$. As shown below, this time is long enough for the instability to occur.

5.3. Seeds of the Filamentation. Let us now calculate the correlation tensor (5.2) for the distribution functions (5.3),(5.4). Due to the symmetry $f(\mathbf{p}) = f(-\mathbf{p})$ of these distributions, the tensor $M^{\mu\nu}$ is diagonal, i.e., $M^{\mu\nu} = 0$ for $\mu \neq \nu$. Since the average parton longitudinal momentum is much bigger than the transverse one, it obviously follows from Eq. (5.2) that the largest fluctuating current appears along the z axis. Therefore, we discuss the M^{zz} component of the correlation tensor. $M^{zz}(\omega, \mathbf{k})$ depends on the $\mathbf{k}$-vector orientation and there are two generic cases: $\mathbf{k} = (k_x, 0, 0)$ and $\mathbf{k} = (0, 0, k_z)$. The inspection of Eq. (5.2) shows that the fluctuations with $\mathbf{k} = (k_x, 0, 0)$ are much larger than those with $\mathbf{k} = (0, 0, k_z)$. Thus, let us consider $M^{zz}(\omega, k_x)$. Substituting the distributions (5.3), (5.4) into (5.2) one finds after azimuthal integration that $M^{zz}_{ab}(\omega, k_x)$ reaches the maximal values for $\omega^2 \ll k_x^2$. So, we compute M^{zz}_{ab} at $\omega = 0$. Keeping in

mind that $e^Y \gg 1$ and $\mathcal{P} \gg \langle p_\perp \rangle$ we get the following approximate expressions for the flat y- and $p_\parallel$ distributions:

$$M^{zz}_{ab}(\omega = 0, k_x) = \frac{1}{8}\, g^2\, \delta^{ab}\, \frac{e^Y}{Y}\, \frac{\langle \rho \rangle}{|k_x|}\,, \tag{5.5}$$

$$M^{zz}_{ab}(\omega = 0, k_x) = \frac{1}{8}\, g^2\, \delta^{ab}\, \frac{\mathcal{P}}{\langle p_\perp \rangle}\, \frac{\langle \rho \rangle}{|k_x|}\,, \tag{5.6}$$

where $\langle \rho \rangle$ is the effective parton density given for $N_c = 3$ as

$$\langle \rho \rangle \equiv \int \frac{d^3p}{(2\pi)^3}\, f(\mathbf{p}) = \frac{1}{4\pi^2} \int_0^\infty dp_\perp p_\perp\, h(p_\perp) = \frac{1}{3}\, \langle \rho \rangle_{q\bar{q}} + \frac{3}{4}\, \langle \rho \rangle_g\,,$$

with $\langle \rho \rangle_{q\bar{q}}$ denoting the average density of quarks and antiquarks, and $\langle \rho \rangle_g$ that of gluons. For the flat $p_\parallel$ case we have also used the approximate equality

$$\int_0^\infty dp_\perp\, h(p_\perp) \cong \frac{1}{\langle p_\perp \rangle} \int_0^\infty dp_\perp p_\perp\, h(p_\perp)$$

to get the expression (5.6). It is instructive to compare the results (5.5), (5.6) with the analogous one for the equilibrium plasma which is

$$M^{zz}_{ab}(\omega = 0, k_x) = \frac{\pi}{16}\, g^2\, \delta^{ab}\, \frac{\langle \rho \rangle}{|k_x|}\,.$$

One sees that the current fluctuations in the anisotropic plasma are amplified by the *large* factor which is e^Y/Y or $\mathcal{P}/\langle p_\perp \rangle$. With the estimated value of Y 2.5 for RHIC and 5.0 for LHC [74], the amplification factor e^Y/Y equals 4.9 and 29.7, respectively.

5.4. Filamentation Mechanism. Following [75] we are going to argue that the fluctuation, which contributes to $M^{zz}_{ab}(\omega = 0, k_x)$, grows in time. The form of the fluctuating current is

$$\mathbf{j}_a(x) = j_a\, \hat{\mathbf{e}}_z \cos(k_x x)\,, \tag{5.7}$$

where $\hat{\mathbf{e}}_z$ is the unit vector in the z direction. Thus, there are current filaments of the thickness $\pi/|k_x|$ with the current flowing in the opposite directions in the neighboring filaments. For the purpose of a qualitative argumentation presented here the chromodynamics is treated as an eightfold electrodynamics. Then, the magnetic field generated by the current (5.7) is given as

$$\mathbf{B}_a(x) = \frac{j_a}{k_x}\, \hat{\mathbf{e}}_y \sin(k_x x)\,,$$

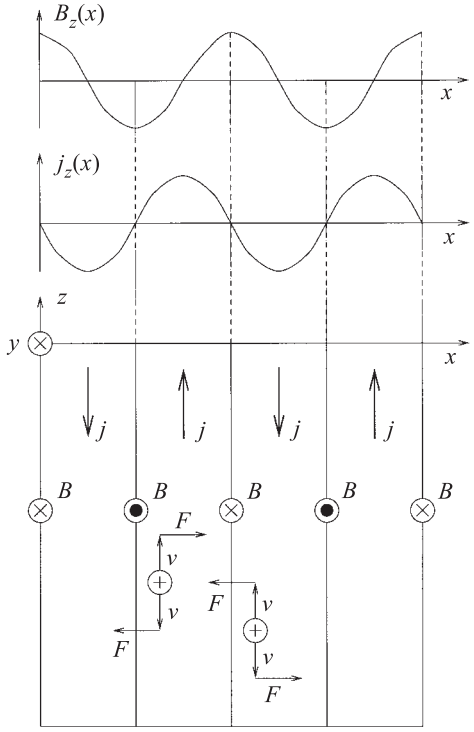

Fig. 4. The mechanism of filamentation. The phenomenon is, for simplicity, considered in terms of the electrodynamics. The fluctuating current generates the magnetic field acting on the positively charged particles which in turn contribute to the current (see text). $\otimes$ and $\odot$ denote the parallel and, respectively, antiparallel orientation of the magnetic field with respect to the y-axis

while the Lorentz force acting on the partons, which fly along the beam, equals

$$\mathbf{F}(x) = q_a\,\mathbf{v} \times \mathbf{B}_a(x) = --\,q_a\,v_z\,\frac{j_a}{k_x}\,\hat{\mathbf{e}}_x \sin(k_x x)\ ,$$

where q_a is the color charge. One observes, see Fig. 4, that the force distributes the partons in such a way that those, which positively contribute to the current in a given filament, are focused to the filament centre while those, which negatively contribute, are moved to the neighboring one. Thus, the initial current grows.

5.5. Dispersion Equation. We analyse here the dispersion equation which for the anisotropic plasma is of the form (4.14). The plasma is assumed to be collisionless, i.e., the mean-field interaction dominates the system dynamics and $\nu = i0^+$. The assumption is correct if the inverse characteristic time of the

mean-field phenomena τ^{-1} is substantially larger than the collision frequency ν. Otherwise, the infinitesimally small imaginary quantity $i0^+$ from (4.12) should be substituted by $i\nu$. Such a substitution however seriously complicates analysis of the dispersion equation (4.14). Therefore, we solve the problem within the collisionless limit and only *a posteriori* argue validity of this approximation.

As already mentioned, the solutions $\omega(\mathbf{k})$ of (4.14) are stable when $\mathrm{Im}\omega < 0$ and unstable when $\mathrm{Im}\omega > 0$. It appears difficult to find the solutions of Eq. (4.14) because of the complicated structure of the chromodielectric tensor (4.12). However, the problem simplifies because we are interested in the specific modes with the wave vector $\mathbf{k}$ perpendicular and to the chromoelectric field $\mathbf{E}$ parallel to the beam. Thus, we consider the configuration

$$\mathbf{E} = (0, 0, E_z) \ , \quad \mathbf{k} = (k_x, 0, 0) \ . \tag{5.8}$$

Then, the dispersion equation (4.14) gets the form

$$H(\omega) \equiv k_x^2 - \omega^2 \epsilon^{zz}(\omega, k_x) = 0 \ , \tag{5.9}$$

where only one diagonal component of the dielectric tensor enters.

5.6. Penrose Criterion. The stability analysis can be performed without solving Eq. (5.9) explicitly. Indeed, the so-called Penrose criterion [76] states that *the dispersion equation* $H(\omega) = 0$ *has unstable solutions if* $H(\omega = 0) < 0$. The meaning of this statement will be clearer after we will approximately solve the dispersion equation in the next section.

Let us compute $H(0)$ which can be written as

$$H(0) = k_x^2 - \chi^2 \ , \tag{5.10}$$

with

$$\chi^2 \equiv -\omega_0^2 - \frac{g^2}{2} \int \frac{d^3p}{(2\pi)^3} \ \frac{v_z^2}{v_x} \ \frac{\partial f(\mathbf{p})}{\partial p_x} \ , \tag{5.11}$$

where the plasma frequency parameter is

$$\omega_0^2 \equiv -\frac{g^2}{2} \int \frac{d^3p}{(2\pi)^3} \ v_z \ \frac{\partial f(\mathbf{p})}{\partial p_z} \ . \tag{5.12}$$

As we shall see below, ω_0 gives the frequency of the stable mode of the configuration (5.8) when $k_x \to 0$.

Substituting the distribution functions (5.3), (5.4) into Eqs. (5.11) and (5.12) one finds the analytical but rather complicated expression of $H(0)$. In the case of the flat y distribution we thus take the limit $e^Y \gg 1$, while for the flat $p_\parallel$ distribution we assume that $\mathcal{P} \gg \langle p_\perp \rangle$. Then, we get for the flat y distribution

$$\chi^2 \cong -\frac{\alpha_s}{4\pi} \ \frac{e^Y}{Y} \ \int dp_\perp \left(h(p_\perp) + p_\perp \frac{dh(p_\perp)}{dp_\perp} \right) = \frac{\alpha_s}{4\pi} \ \frac{e^Y}{Y} \ p_\perp^{\min} h(p_\perp^{\min}) \ , \tag{5.13}$$

and for the flat $p_\parallel$ distribution

$$\chi^2 \cong -\frac{\alpha_s}{4\pi}\,\mathcal{P}\int dp_\perp \frac{dh(p_\perp)}{dp_\perp} = \frac{\alpha_s}{4\pi}\,\mathcal{P}\,h(p_\perp^{\min})\,, \tag{5.14}$$

where $\alpha_s \equiv g^2/4\pi^2$ is the strong coupling constant and $p_\perp^{\min}$ denotes the minimal transverse momentum. The function $h(p_\perp)$ is assumed to decrease faster than $1/p_\perp$ when $p_\perp \to \infty$.

As seen, the sign of $H(0)$ given by Eq. (5.10) is (for sufficiently small k_x^2) determined by the transverse momentum distribution at the minimal momentum. There are unstable modes if $p_\perp^{\min} h(p_\perp^{\min}) > 0$ for the flat y distribution and if $h(p_\perp^{\min}) > 0$ for the flat $p_\parallel$ case. Since the distribution $h(p_\perp)$ is expected to be a monotonously decreasing function of $p_\perp$, the instability condition for the flat $p_\parallel$ distribution seems to be always satisfied. The situation with the flat y distribution is less clear. So, let us discuss it in more detail. We consider three characteristic cases of $h(p_\perp)$ discussed in the literature.

1. The transverse momentum distribution due to a single binary parton-parton interaction is proportional to $p_\perp^{-6}$ [77] and blows up when $p_\perp \to 0$. In such a case $p_\perp^{\min} h(p_\perp^{\min}) > 0$, there are unstable modes and $p_\perp^{\min}$ should be treated as a cut-off parameter reflecting, e.g., the finite size of the system.

2. The transverse momentum distribution proportional to $(p_\perp + m_\perp)^{-6.4}$ with $m_\perp = 2.9$ GeV has been found in [74], where except the binary parton-parton scattering the initial and final state radiation has been taken into account. This distribution, in contrast to that from 1), gives $p_\perp^{\min} h(p_\perp^{\min}) = 0$ for $p_\perp^{\min} = 0$ and there is no instability. Although one should remember that the finite value of $m_\perp$ found in [74] is the result of infrared cut-off. Thus, it seems more reasonable to use the distribution from 1), where the cut-off explicitly appears.

3. One treats perturbatively only partons with $p_\perp > p_\perp^{\min}$ assuming that those with lower momenta form colorless clusters or strings due to a nonperturbative interaction. It should be stressed that the colorless objects do not contribute to the dielectric tensor (4.12), which is found in the *linear* response approximation [7,66]. Thus, only the partons with $p_\perp > p_\perp^{\min}$ are of interest for us. Consequently $p_\perp^{\min} h(p_\perp^{\min})$ is positive and there are unstable modes. As shown in [72], the screening lengths due to the large parton density are smaller than the confinement scale in the vacuum. Therefore, the cut-off parameter $p_\perp^{\min}$ should be presumably reduced from 1 — 2 GeV usually used for proton–proton interactions to, let us say, 0.1 — 0.2 GeV.

We cannot draw a firm conclusion but we see that the instability condition is trivially satisfied for the flat $p_\parallel$ distribution and is also fulfilled for the flat

y distribution under plausible assumptions. Let us mention that the difference between the instability conditions for the flat y and $p_\parallel$ distribution is due to a very specific property of the y distribution which is limited to the interval $(-Y, Y)$. The point is that $y \to \pm\infty$ when $p_\perp \to 0$ and consequently, the limits in the rapidity suppress the contribution from the small transverse momenta to the dielectric tensor. For this reason we need for the instability the distribution $h(p_\perp)$ which diverges for $p_\perp \to 0$ in the case of the flat y distribution, while the instability condition for the flat $p_\parallel$ distribution is satisfied when $h(0)$ is finite. If we assumed the Gaussian rapidity distribution instead of (5.3), the instability condition would be less stringent. In any case, we assume that the Penrose criterion is satisfied and look for the unstable modes solving the dispersion equation (5.9).

5.7. Unstable Mode. The dispersion equation (5.9) for a cylindrically symmetric system is

$$\begin{aligned} k_x^2 - \omega^2 + \omega_0^2 \quad &- \quad \frac{\alpha_s}{4\pi^2} \int_0^\infty dp_\perp \int_{-\infty}^\infty \frac{dp_\parallel \, p_\parallel^2}{\sqrt{p_\parallel^2 + p_\perp^2}} \\ &\times \quad \frac{\partial f}{\partial p_\perp} \int_0^{2\pi} \frac{d\phi \, \cos\phi}{a - \cos\phi + i0^+} = 0 \, , \end{aligned} \tag{5.15}$$

with the plasma frequency ω_0 given by Eq. (5.12) and a denoting

$$a \equiv \frac{\omega}{k_x} \, \frac{\sqrt{p_\parallel^2 + p_\perp^2}}{p_\perp} \, .$$

We solve Eq. (5.15) in the two limiting cases $|\omega/k_x| \gg 1$ and $|k_x/\omega| \gg 1$. In the first case the azimuthal integral is approximated as

$$\int_0^{2\pi} \frac{d\phi \, \cos\phi}{a - \cos\phi + i0^+} = \frac{\pi}{a^2} + \mathcal{O}(a^{-4}) \, .$$

Then, the equation (5.15) gets the form

$$k_x^2 - \omega^2 + \omega_0^2 + \eta^2 \frac{k_x^2}{\omega^2} = 0 \, , \tag{5.16}$$

where η, as ω_0, is a constant defined as

$$\eta_0^2 \equiv -\frac{\alpha_s}{4\pi} \int dp_\parallel dp_\perp \frac{p_\parallel^2 p_\perp^2}{(p_\parallel^2 + p_\perp^2)^{3/2}} \frac{\partial f(\mathbf{p})}{\partial p_\perp} \, .$$

We have computed ω_0 and η for the flat $p_\parallel$- and y distribution. In the limit $e^Y \gg 1$ and $\mathcal{P} \gg \langle p_\perp \rangle$, respectively, we have found

$$\omega_0^2 \cong \frac{\alpha_s}{8Y} \int dp_\perp h(p_\perp) \, , \tag{5.17}$$

$$\omega_0^2 \cong \frac{\alpha_s}{2\pi\mathcal{P}} \int dp_\perp p_\perp h(p_\perp) \,, \tag{5.18}$$

and

$$\eta^2 \cong \frac{\alpha_s}{16Y} \int dp_\perp \left(\frac{1}{4} h(p_\perp) - p_\perp \frac{dh(p_\perp)}{dp_\perp} \right) , \tag{5.19}$$

$$\eta^2 \cong -\frac{\alpha_s}{4\pi\mathcal{P}} \ln\left(\frac{\mathcal{P}}{\langle p_\perp \rangle} \right) \int dp_\perp p_\perp^2 \frac{dh(p_\perp)}{dp_\perp} \,. \tag{5.20}$$

The solutions of Eq. (5.16) are

$$\omega_\pm^2 = \frac{1}{2}\Big(k^2 + \omega_0^2 \pm \sqrt{(k_x^2 + \omega_0^2)^2 + 4\eta^2 k_x^2} \Big) \,. \tag{5.21}$$

One sees that $\omega_+^2 \geq 0$ and $\omega_-^2 \leq 0$. Thus, there is a pure real mode ω_+, which is stable, and two pure imaginary modes ω_-, one of them being unstable. As mentioned previously, $\omega_+ = \omega_0$ when $k_x = 0$.

Let us focus our attention on the unstable mode which can be approximated as

$$\omega_-^2 \cong \begin{cases} -\frac{\eta^2}{\omega_0^2} k_x^2 \,, & \text{for} \quad k_x^2 \ll \omega_0^2 \\ -\eta^2 \,, & \text{for} \quad k_x^2 \gg \omega_0^2. \end{cases}$$

One should keep in mind that Eq. (5.21) holds only for $|\omega/k_x| \gg 1$. We see that ω_- can satisfy this condition for $k_x^2 \ll \omega_0^2$ if $\eta^2 \gg \omega_0^2$ and for $k_x^2 \gg \omega_0^2$ if $\eta^2 \ll \omega_0^2$. To check whether these conditions can be satisfied, we compare η^2 to ω_0^2. Assuming that $h(p_\perp) \sim p_\perp^{-\beta}$, one finds from Eqs. (5.19), (5.20)

$$\eta^2 \cong \frac{1+4\beta}{8} \, \omega_0^2 \,, \tag{5.22}$$

$$\eta^2 \cong \frac{\beta}{2} \ln\left(\frac{\mathcal{P}}{\langle p_\perp \rangle} \right) \omega_0^2 \,.$$

Since $\beta \cong 6$ [74,77] we get $\eta^2 \geq 3\omega_0^2$. Therefore, the solution (5.21) for $k_x^2 \ll \omega_0^2$ should be correct.

Let us now solve the dispersion equation (5.15) in the second case when $|k_x/\omega| \gg 1$. Then, the azimuthal integral from Eq. (5.15) is approximated as

$$\int_0^{2\pi} \frac{d\phi \, \cos\phi}{a - \cos\phi + i0^+} = -2\pi + \mathcal{O}(a) \,,$$

and we immediately get the dispersion relation

$$\omega^2 = k_x^2 - \chi^2 \,, \tag{5.23}$$

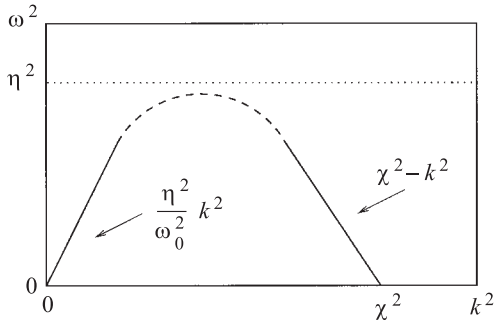

Fig. 5. The schematic view of the dispersion relation of the filamentation mode

with χ^2 given by Eq. (5.13) or (5.14). As previously we have assumed that $e^Y \gg 1$ and $\mathcal{P} \gg \langle p_\perp \rangle$. Eq. (5.23) provides a real mode for $k_x^2 > \chi^2$ and two imaginary modes for $k_x^2 < \chi^2$. Since the solution (5.23) must satisfy the condition $|k_x/\omega| \gg 1$, it holds only for $k_x^2 \gg |k_x^2 - \chi^2|$.

The dispersion relation of the unstable mode in the whole domain of wave vectors is schematically shown in Fig. 5, where the solutions (5.21) and (5.23) are combined. Now one sees how the Penrose criterion works. When $\chi^2 = 0$, the unstable mode disappears.

5.8. Time Scales. The instability studied here can occur in heavy-ion collisions if the time of instability development is short enough, shorter than the characteristic time of evolution of the nonequilibrium state described by the distribution functions (5.3), (5.4).

Let us first estimate the time of instability development which is given by $1/\mathrm{Im}\omega$. As is seen in Fig. 5, $|\mathrm{Im}\omega| < \eta$. Thus, we define the minimal time as $\tau_{\min} = 1/\eta$. To find $\tau_{\min}$ we estimate the plasma frequency. We consider here only the flat y distribution which seems to be more reasonable than the flat $p_\parallel$ distribution. Approximating $\int dp_\perp h(p_\perp)$ as $\int dp_\perp p_\perp h(p_\perp)/\langle p_\perp \rangle$ the plasma frequency (5.12) can be written as

$$\omega_0^2 \cong \frac{\alpha_s \pi}{6 Y r_0^2 A^{2/3}} (N_q + N_{\bar{q}} + \frac{9}{4} N_g) \,, \tag{5.24}$$

where $N_c = 3$; N_q, $N_{\bar{q}}$, and N_g are the numbers of quarks, antiquarks and gluons, respectively, produced in the volume, which has been estimated in the following way. Since we are interested in the central collisions, the volume corresponds to a cylinder of the radius $r_0 A^{1/3}$ with $r_0 = 1.1$ fm and A being the mass number of the colliding nuclei. Using the uncertainty principle argument, the length of the cylinder has been taken as $1/\langle p_\perp \rangle$, which is the formation time of parton with the transverse momentum $\langle p_\perp \rangle$.

Neglecting quarks and antiquarks in Eq. (5.24) and substituting there $N_g = 570$ for the central Au–Au collision at RHIC ($Y = 2.5$) and $N_g = 8100$ for the same colliding system at LHC ($Y = 5.0$) [74], we get

$$\omega_0 = 280 \ \text{MeV} \quad \text{for RHIC}\,, \qquad \omega_0 = 430 \ \text{MeV} \quad \text{for LHC}$$

for $\alpha_s = 0.3$ at RHIC and $\alpha_s = 0.1$ at LHC. Using Eq. (5.22) with $\beta = 6$ one finds

$$\tau_{\min} = 0.4 \ \text{fm}/c \quad \text{for RHIC}\,, \qquad \tau_{\min} = 0.3 \ \text{fm}/c \quad \text{for LHC}\,.$$

The plasma has been assumed collisionless in our analysis. Such an assumption is usually correct for weakly interacting systems because the damping rates of the collective modes due to collisions are of the higher order in α_s than the frequencies of these modes, see, e.g., [61]. However, it has been argued recently [78] that the color collective modes are overdamped due to the unscreened chromomagnetic interaction. However it is unclear whether these arguments concern the unstable mode discussed here. The point is that the paper [78] deals with the neutralization of color charges which generate the longitudinal chromoelectric field while the unstable mode which we have found is transversal and consequently is generated by the color currents not charges. Let us refer here to the electron-ion plasma, where the charge neutralization is a very fast process while currents can exist in the system for a much longer time [76]. In any case, the above estimates of the instability development should be treated as lower limits.

Let us now discuss the characteristic time of evolution of the nonequilibrium state described by the distribution functions (5.3), (5.4). Except the possible unstable collective modes, there are two other important processes responsible for the temporal evolution of the initially produced many-parton system: free streaming [79–81] and parton–parton scattering. The two processes lead to the isotropic momentum distribution of partons in a given cell. The estimated time to achieve local isotropy due to the free streaming is about 0.7 fm/c at RHIC [81]. The estimates of the equilibration time due to the parton scatterings are similar [82, 83]. As is seen the three-time scales of interest are close to each other. Therefore, the color unstable modes can play a role in the dynamics of many-parton system produced at the early stage of heavy-ion collision, but presumably the pattern of instability cannot fully develop.

5.9. Detecting the Filamentation. One asks whether the color instabilities are detectable in ultrarelativistic heavy-ion collisions. The answer seems to be positive because the occurrence of the filamentation breaks the azimuthal symmetry of the system and hopefully will be visible in the final state. The azimuthal orientation of the wave vector will change from one collision to another while the instability growth will lead to the energy transport along this vector (the Poynting vector points in this direction). Consequently, one expects significant

variation of the transverse energy as a function of the azimuthal angle. This expectation is qualitatively different than that based on the parton cascade simulations [59], where the fluctuations are strongly damped due to the large number of uncorrelated partons. Due to the collective character of the filamentation instability the azimuthal symmetry will be presumably broken by a flow of large number of particles with relatively small transverse momenta. The jets produced in hard parton-parton interactions also break the azimuthal symmetry. However, the symmetry is broken in this case due to a few particles with large transverse momentum. The problem obviously needs further studies but the event-by-event analysis of the nuclear collision seems to give a chance to observe the color instabilities in the experiments planed at RHIC and LHC.

REFERENCES

1. **Yndurain F.J.**, — Quantum Chromodynamics. Springer, New York, 1983.
2. Proc. of Int. Conf. on Ultrarelativistic Nucleus-Nucleus Collisions, Quark Matter'96, Heidelberg, 1996, edited by Braun-Munzinger P., H.J. Specht H.J., Stock R. and Stöcker H. North-Holland, Amsterdam, 1996; Nucl. Phys., 1996, v.A610.
3. **deGroot S.R., van Leeuwen W.A., van Weert Ch. G.** — Relativistic Kinetic Theory. North-Holland, Amsterdam, 1980.
4. **Elze H.-Th., Heinz U.** — Phys. Rep., 1989, v.183, p.81.
5. **Blaizot J.-P., Iancu E.** — Nucl. Phys., 1994 v.B417, p.608.
6. **Kalashnikov O.K.** — Fortschritte Phys., 1984, v.32, p.525.
7. **Mrówczyński St.** — Phys. Rev., 1989, v.D39, p.1940.
8. **Kelly P.F., Liu Q., Lucchesi C., Manuel C.** — Phys. Rev., 1994, v.D50, p.4209.
9. **Markov Yu.A., Markova M.A.** — Teor. Mat. Fiz., 1996, v.108. p.159 (in Russian).
10. **Markov Yu.A., Markova M.A.** — Teor. Mat. Fiz., 1997, v.111, p.263 (in Russian).
11. **Braaten E., Pisarski R. D.** — Nucl. Phys., 1990, v.B337, p.569.
12. **Selikhov A. V.** — Phys. Lett., 1991, v.B268, p.263.
13. **Selikhov A. V., Gyulassy M.** — Phys. Rev., 1994, v.C49, p.1726.
14. **Geiger K.** — Phys. Rev., 1996, v.D54, p.949.
15. **Markov Yu.A., Markova M.A.** — Teor. Mat. Fiz., 1995, v.103, p.123 (in Russian).
16. **Schwinger J.** — Phys. Rev., 1951, v.82, p.664.
17. **Bialas A., Czyż W.** — Acta Phys. Pol., 1986, v.B17, p.635.
18. **Gatoff G., Kerman A.K., Matsui T.** — Phys. Rev., 1987, v.D36, p.114.
19. **Cooper F.** et al. — Phys Rev., 1993, v.D48, p.190.
20. **Kluger Y., Eisenberg J.M., Svetitsky B.** — Int. J. Mod. Phys., 1993, v.E2, p.333.
21. **Rau J., Müller B.** — Phys. Rep., 1996, v.272, p.1.
22. **Schmidt S.** et al., hep-ph/9809227, Int. J. Mod. Phys. E (in print).
23. **Schwinger J.** — J. Math. Phys., 1961, v.2, p.407.

24. **Keldysh L.V.** — Zh. Eksp. Teor. Fiz., 1964, v.47, p.1515.
25. **Kadanoff L.P., Baym G.** — Quantum Statistical Mechanics. Benjamin, New York, 1962.
26. **Bezzerides B., Dubois D.F.** — Ann. Phys., 1972, v.70, p.10.
27. **Li S.-P., L. McLerran L.** — Nucl. Phys., 1983, v.B214, p.417.
28. **Danielewicz P.** — Ann. Phys. (N.Y.), 1984, v.152, p.239.
29. **Calzetta E., Hu B. L.** — Phys. Rev., 1988, v.D37, p.2878.
30. **Mrówczyński St., Danielewicz P.** — Nucl. Phys., 1990, v.B342, p.345.
31. **Mrówczyński St., Heinz U.** — Ann. Phys., 1994, v.229, p.1.
32. **Henning P.** — Phys. Rep., 1995, v.253, p.235.
33. **Boyanowsky D., Lawrie I.D., Lee D.-S.** — Phys. Rev., 1996, v.D54, p.4013.
34. **Klevansky S.P., Ogura A., Hüfner J.** — Ann. Phys., 1997, v.261, p.37.
35. **Rehberg P.** — Phys. Rev., 1998, v.C57, p.3299.
36. **Mrówczyński St.** — Phys. Rev., 1997, v.D56, p.2265.
37. **Henning P.** — Nucl. Phys., 1990, v.B337, p.547.
38. **Bjorken J. D., Drell S. D.** — Relativistic Quantum Fields. McGraw-Hill, San Francisco, 1964.
39. **Nordheim L.W.** — Proc. Roy. Soc. (London), 1928, v.A119, p.689.
40. **Uehling E.A., Uhlenbeck G.E.** — Phys. Rev., 1933, v.43, p.552.
41. **Heinz U.** — Phys. Rev. Lett., 1983, v.51, p.351.
42. **Winter J.** — J. Phys. (Paris), 1984, v.45, C6, p.53.
43. **Elze H.-Th., Gyulassy M., Vasak D.** — Nucl. Phys., 1986, v.B276, p.706.
44. **Elze H.-Th., Gyulassy M., Vasak D.** — Phys. Lett., 1986, v.B177, p.402.
45. **Landau L.D., Lifshitz E.M.** — Electrodynamics of Continuous Media. Pergamon, New York, 1960.
46. **Silin V.P., Ruhadze A.A.** — Electrodynamics of Plasma, Plasma-Like Media. Gosatomizdat, Moscow, 1961 (in Russian).
47. **Lifshitz E.M., Pitaevskii L.P.** — Physical Kinetics, Pergamon, New York, 1981.
48. **Elze H.-Th.** — Z. Phys., 1987, v.C38, p.211.
49. **Heinz U., Siemens P.J.** — Phys. Lett., 1985, v.B158, p.11.
50. **Heinz U.** — Ann. Phys., 1986, v.168, p.148.
51. **Mrówczyński St.** — Phys. Lett., 1987, v.B188, p.129.
52. **Bialas A., Czyż W.** — Ann. Phys., 1988, v.187, p.97.
53. **Bialas A., Czyż W., Dyrek A., Florkowski W.** — Nucl. Phys., 1988, v.B296, p.611.
54. **Heinz U.** — Ann. Phys., 1985, v.161, p.48.
55. **Weldon H.A.** — Phys. Rev., 1982, v.D26, p.1394.
56. **Hansson T.H., Zahed I.** — Nucl. Phys., 1987, v.B292, p.725.
57. **Heinz U., Kajantie K., Toimela T.** — Ann. Phys., 1987, v.176, p.218.
58. **Weldon H.A.** — Phys. Rev., 1983, v.D28, p.2007.
59. **Geiger K.** — Phys. Rep., 1995, v.258, p.237.

60. **Wang X.-N.** — Phys. Rep., 1997, v.280, p.287.
61. **A.I. Akhiezer** et al. — Plasma Electrodynamics. Pergamon, New York, 1975.
62. **Heinz U.** — Nucl. Phys., 1984, v.A418, p.603c.
63. **Ivanov Yu.B.** — Nucl. Phys., 1987, v.A474, p.693.
64. **Henning P., Friman B.L.** — Nucl. Phys., 1988, v.A490, p.689.
65. **Pokrovskii Yu. E., Selikhov A.V.** — Pis'ma Zh. Eksp. Teor. Fiz., 1988, v.47 p.11.
66. **Mrówczyński St.** — Phys. Lett., 1988, v.B214, p.587.
67. **Pokrovskii Yu. E., Selikhov A.V.** — Yad. Fiz., 1990, v.52, p.229.
68. **Pokrovskii Yu. E., Selikhov A.V.** — Yad. Fiz., 1990, v.52, p.605.
69. **Pavlenko O.P.** — Yad. Fiz., 1992, v.55, p.2239.
70. **Weibel E.S.** — Phys. Rev. Lett., 1959, v.2, p.83.
71. **Mrówczyński St.** — Phys. Lett., 1993, v.B314, p.118.
72. **Mrówczyński St.** — Phys. Rev., 1994, v.C49, p.2191.
73. **Mrówczyński St.** — Phys. Lett., 1997, v.B393, p.26.
74. **Biró T.S., Müller B., Wang X.-N.** — Phys. Lett., 1992, v.B283, p.171.
75. **Chen F.F.** — Introduction to Plasma Physics and Controlled Fusion. Plenum Press, New York, 1984.
76. **Krall N.A., Trivelpiece A.W.** — Principles of Plasma Physics. McGraw-Hill, New York, 1973.
77. **Eskola K.J., Kajantie K., Lindfors J.** — Nucl. Phys., 1989, v.B323, p.37.
78. **Gyulassy M., Selikhov A.V.** — Phys. Lett., 1993, v.B316, p.373.
79. **Hwa R., Kajantie K.** — Phys. Rev. Lett., 1986, v.56, p.696.
80. **Biró T.S.** et al. — Phys. Rev.,1993, v.C48, p.1275.
81. **Eskola K.J., Wang X.-N.** — Phys. Rev., 1993, v.C47, p.2329.
82. **Geiger K.** — Phys. Rev.,1992, v.D46, p.4986.
83. **Shuryak E.** — Phys. Rev. Lett., 1992, v.68, p.3270.